3-REVOLUTE ORIENTATION SENSING MECHANISM

A PROJECT REPORT

Submitted by

BL.EN.U4MEE13107	SHASA A.ANTAO
BL.EN.U4MEE13074	VISHNU S.NAIR
BL.EN.U4MEE13095	RAGUL P.

in partial fulfillment for the award of the degree Of

BACHELOR OF TECHNOLOGY

IN

MECHANICAL ENGINEERING

AMRITA SCHOOL OF ENGINEERING, BANGALORE

AMRITA VISHWA VIDYAPEETHAM

BANGALORE 560 035

May-2017

AMRITA VISHWA VIDYAPEETHAM
AMRITA SCHOOL OF ENGINEERING, BANGALORE, 560035

BONAFIDE CERTIFICATE

This is to certify that the project report entitled "**3-REVOLUTE ORIENTATION SENSING MECHANISM"** submitted by

SHASA A. ANTAO	BL.EN. U4MEE13107
VISHNU S. NAIR	BL.EN. U4MEE13074
RAGUL P.	BL.EN. U4MEE13095

In partial fulfillment of the requirements for the award of the degree **Bachelor of Technology** in **MECHANICAL ENGINEERING** is a bonafide record of the work carried out under my guidance and supervision at Amrita School of Engineering, Bangalore.

Mr. Rajeevlochana G. Chittawadigi
Asst. Professor
Mechanical Engineering

Dr. T. Srinivas Rao
Asso. Professor
Mechanical Engineering

Dr. Nagaraja S.R
Chairperson
Mechanical Engineering

This project report was evaluated by us on ……

INTERNAL EXAMINER

EXTERNAL EXAMINER

Acknowledgement

First and foremost, we would like to thank our beloved Amma, Mata Amritanandamayi Devi for her blessings.

We wish to place on record our sincere thanks to **Dr. Rakesh S.G**, Associate Dean, Amrita Vishwa Vidyapeetham, Bangalore, for having permitted us to undertake this work. We wish to thank **Dr. Nagaraja S.R**, Chairperson, Department of Mechanical Engineering, Amrita Vishwa Vidyapeetham, Bangalore, for providing this opportunity for us and for supporting us every step of the way. We would like to thank our guide, **Mr. Rajeevlochana G. Chittawadigi**, Asst. Professor, Department of Mechanical Engineering for his constant guidance, steadfast support and encouragement that have been instrumental in ensuring that we worked sincerely and efficiently. We would like to express our sincere thanks to **Dr. T. Srinivas Rao**, Asso. Professor Department of Mechanical Engineering and **Mr. Ravi Kumar V.**, Asst. Professor, Department of Mechanical Engineering, for his support in every possible manner throughout this course.

We would also like to thank **Mr. Dharmendra** and **Mr. Lakshmi Narayana**, Laboratory Staff, Department of Mechanical Engineering, Amrita Vishwa Vidyapeetham, Bangalore for their constant support.

Last but not the least, we would like to thank **Mr. Argenio Antao**, who with his experience and knowledge guided us through the fabrication process. We would also like to thank our families for their support in the completion of this project and also our student friends without whose good wishes this project could not have been successfully completed.

Abstract

In the field of robotics, several instances exist when the orientation of an object has to be controlled. It can be done using input devices such as a joystick or a 3D mouse. In this project, a novel serial chain mechanism named as the 3-R Orientation Sensing Mechanism (3-ROSM) is presented, which consists of 3-Revolute joints that intersect at the center of the object to be held by the user. The mechanism has extensions in two links to place counterweights for passive balancing, such that the mechanism would remain at a configuration as left by the user after using it. As the configuration of the links change according to the user's input, the mechanism should be designed such that the overall centre of gravity remains constant. The centre of gravity of the links, which are a combination of primitive shapes, can be found theoretically using the size and density of the material of the links. However, it could have some inaccuracies due to machining process. Hence a method, referred to as the Hanging Method, was used to find the CG of the links with respect to a predetermined coordinate frame. The characteristic feature of this mechanism is that the three axes of the links are intersecting as found in various Gimbal linkage systems. The balancing is carried out using counterweights placed on linkages on the moving links. The T-shaped extensions have threaded portions on them such that the placement of the counterweights, similar to a nut fastener, can be modified whenever required. This allows infinite resolution for the accommodation of the counterweights, which is also a novel feature of the 3-ROSM. Hollow shaft encoders are added to the joints to measure the change in orientation angles of the object held by the user. These angles can then be used as an input to control the orientation of another object. The end result is a mechanism that can be used as a hand operated balanced mechanism (HOBM) in applications such as tele-surgery; control of a CCTV camera mounted on a Gimbal mechanism, etc., which utilize master-slave robotics as a principle. To demonstrate its usability, a 3-axis camera mount is designed and then controlled using the 3-ROSM.

Table of Contents

List of Figures

List of Tables

List of Symbols, Abbreviations and Nomenclatures

3-ROSM – 3 Revolute Orientation Sensing Mechanism

CAD Software – Computer Aided Design Software

3D – 3 Dimension

DOF – Degree of Freedom

EE – End Effector

k_p – Spring stiffness

T_1 and T_2 – Tension in Fig (2.11)

m – mass

g – acceleration due to gravity

HOBM – Hand Operated Balanced Manipulator

DH parameters – Denavit Hartenberg parameters

HTM – Homogeneous Transformation Matrix

b_i – Joint Offset

θ_i – Joint Angle

α_i – Link Length

α_i – Twist Angle

T – Homogeneous Transformation Matrix

CG – Centre of Gravity

cm – counterweight annotation

Δ - Difference is length

PLA – PolyLactic Acid

FDM – Fused Deposit Modelling

SLA - StereoLithography

SLS – Selective Laser Sintering

V – Voltage

R – Resistance

GND – Ground connection

1.Introduction

A robot is a machine capable of carrying out a complex series of actions automatically. Robots can be controlled by an external control device called a Controller or the control may be embedded within. A robot controller is a combination of hardware and software to program and control the motion of a combination of different joints in a single or multiple robots in order to place the robot manipulator in the user defined position and orientation. A robot manipulator is a device comprising of a series of joints and links, which is used to manipulate materials without direct contact between the user and the work space. These manipulators can be used to perform tasks that are defined in the Cartesian space, whereas the joints or actuators of the robot are generally controlled in the joint space. They can be controlled electronically, using a device called a teach pendent or through the use of switches, joysticks, anthropomorphic harness, or an end effector grip controlled through an offline-programmed computer. The teach pendent controls the manipulator through the use of buttons which allows the user increase or decrease the values of the robot joint angles or move the robot in the Cartesian space directly along the principal directions. However, in this method coordinated end effector motion is difficult, operator response is limited and there is a high probability of the operator to become disoriented. It also lacks force feedback and does not have configuration feedback.

Industrial robots usually consist of a jointed arm (multi-linked manipulator) and an end effector that is attached to a fixed surface. One of the most common type of end effector is a gripper assembly. The robot manipulators can be further classified into serial manipulators and parallel manipulators. Serial manipulators are the most common industrial robots which are designed as a series of links connected by motor-actuated joints that extend from a base to an end-effector. Often they have an anthropomorphic arm structure described as having a "shoulder", an "elbow", and a "wrist". Simplicity considerations in control have led to serial robots with only revolute or prismatic joints and orthogonal, parallel and/or intersecting joint axes. A parallel manipulator is a mechanical system that uses several serial linkage chains to support a single platform or end-effector.

Most of the serial robots used in industries are 6-axis robots which have the last three axes intersecting at a point, known as the wrist of a robot. The first three joint axes

can be actuated to control the position of the end-effector and the last three joint axes can be actuated to control the orientation of the end-effector. Hence, it is better to use two input devices such that the position and orientation can be decoupled for easier control and to increase intuitiveness between the user and the manipulator. In order to control the position of the end-effector of the manipulator, a mechanism which can translate in three orthogonal axes can be used such as the Novint Falcon, which is a delta mechanism with three Degrees of Freedom. To control the three orientation angles of the object, an input device which has three intersecting axes will provide a higher intuitive feeling for the user.

Apart from robots, several other applications exist, wherein control of orientation is an integral part of the functioning of the device. For example, controlling a three-axis camera used for CCTV operations, using an input device to change the viewpoints of a model in a CAD software or in Tele-operation applications which require high accuracy in controlling the orientation of the end-effector. These applications can be classified under Master/Slave robotics which can be defined as a model of transfer of commands in which one device has unidirectional control over the motion of one or more other devices. Master-slave manipulators are general purpose mechanical devices, used by a human operator in a normal environment, to extend his/her hand and arm manipulative capacity into a more-or-less remote hostile environment with the aid of direct (or indirect) visual observation, with movements characterized by naturalness, to obviate the need for extensive training, feel, to reflect the elastic characteristics of task objects and forces exerted on them, and compliance to follow task-constrained paths or orientations at substantial misalignments with operator-applied forces (Jelatis et al. 1975).

This project focuses on control of orientation through Three Degrees of Freedom, through the development of a novel mechanism which is entirely mechanical and does not require motors. It maintains its orientation after the user has left it, through means of passive balancing and also provides a high intuitiveness level between the user and the manipulator, through its innovative design.

2.Literature Review

In the field of robotics, several instances exist when the orientation of an object has to be controlled. These applications determine the type of manipulators to be used and therefore, controllers should be adaptable to changes in application also. As quoted in [11], The designer or supplier of a general purpose programmable robot or manually controlled remote manipulator (tele-operator) has a difficult problem. It is desired that the device fit a great variety of applications, for its very versatility to adapt to whatever specific job the user may have is what makes it economically viable (Sheridan, et.al, 1975). Due to the variety of applications, there is a lack of an exact specification of an objective function or performance criterion. There is a large dependence on the user's ability to accurately assess the specifics of the applications and modify the manipulator or controller, so that it can be applied to its fullest potential.

This problem is addressed by making more advanced controllers while reducing their complexity of use making it easier for the user to adapt. Traditional input devices or mechanisms, such as a joystick or a 3D mouse, utilize sensors or encoders to control the orientation of the manipulator. Hence, accuracy and intuitiveness are imperative in order to successfully make an input device. Exploring purely mechanical input devices reveals several merits such as energy conservation, cost effectiveness, versatility, adaptability etc. Such input mechanisms also simplify complex designs of the robot manipulators they control and with are not inferior to their electronic counterparts in accuracy as well. But, there is a need for external encoders to retrieve data such as joint angles etc. which can otherwise be obtained electronically through the use of servo motors. These servo motors can also bear the load exerted by the joint, eliminating the need for additional balancing techniques to be performed on the input mechanism. However, servo motors are very expensive and are not adaptable in harsh environments and also show poor thermal performance. Therefore, there is a need for accurate and adaptable orientation measurement and as quoted by Antao et al. (2016) For the control of orientation, an input device which has intersecting axes would be ideal and more intuitive.

2.1. Orientation Sensors

As the name suggests orientation sensors are input devices capable of measuring joint angles, primarily through the use of encoders. Geomagic Touch is one such device which can measure both position and orientation of its end-effector. This 6-DOF device is used to manipulate virtual objects and uses haptics which makes it very intuitive. As cited by Suthar et al. (2014) Haptics refers to sensing and manipulation through touch and Haptic feedback provides the operator with a qualitative understanding of changes in the remote environment, especially in situations where visual feedback does not have sufficient resolution.

Space Control 3D Mouse is another device that can be used to take orientation input from user to have applications movement of camera in CAD software, etc. The 3D mouse takes care of positioning the model or view and provides access the application commands as well. The 3D mouse also provides a consistent navigation experience so if more than one 3D application is used, there isn't a need to adjust to different navigation methods as and when applications are switched.

Fig (2.1) Geomagic Touch
(Source Google)

Fig (2.2) Space Control 3D Mouse
(Source space Control)

The Novint Falcon is a desktop haptic robot device which is used to simulate touch in a virtual world, allowing for the "feel" of virtual objects or other physical forces. The Falcon builds on this area of control by providing touch output for the hands. The device consists of three motorized arms attached to an interchangeable end-effector which can be made to simulate various tools with controls of the right type and location. The Falcon's sensors can keep track of the handle's position to sub-millimeter resolution, and the motors are updated 1000 times per second (1 kHz), giving a realistic sense of touch.

The study now shifts onto parallel mechanisms as orientation controllers because they have the characteristics of low inertia, compactness, high rigidity, and precise

resolution as compared to serial mechanisms. However parallel mechanisms are complex and have small workspaces. Therefore, this project studies the various aspects of parallel mechanisms and tries to combine their advantages into a novel serial orientation sensing mechanism by reducing its dependence on joint control via motors and also increasing the overall workspace.

Fig (2.3) Novint Falcon (Source: Google)

Fig (2.4) SHaDe (Birglen et al. 2002)

SHaDe (Spherical Haptic Device) is a 3-DOF mechanism consisting of parallel linkages which can be used in applications involving control of orientation. It consists of a design including only revolute joints with spherical links, i.e. all joint axes intersect at a common point which is the center of rotation of the end effector. This idea of a fixed central point in the end effector is similar to the core theme of this project. As proposed by Birglen et al. (2002) Because of the spherical geometry, such a haptic device has several advantages, namely: pure rotation around a point located inside the user's hand, large workspace and precise manipulation with wrist resting. It is known that in conventional haptic devices, translation is coupled with rotation due to the effect of momentum. In this case a fixed central point, through which the joint axes intersect is designed because it is desired that the haptic controller interface emulate a human wrist. But, although the mechanism has haptic feedback, it has a restricted range of motion.

Yoon et al. (2001) presented a design of a 6-DOF haptic parallel mechanism to interface with virtual reality applications. The mechanism utilizes three ground servomotors

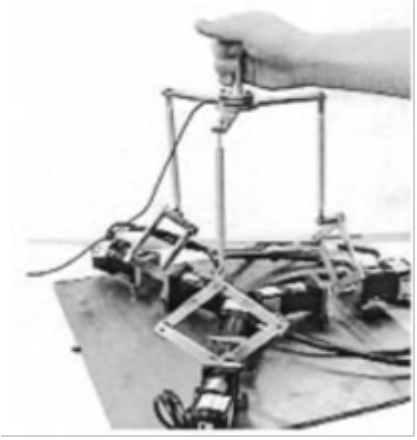

Fig (2.5) 6-DOF haptic parallel mechanism (Yoon et al. 2001)

Fig (2.6) Compact 6-DOF Controller (Tsumaki et al. 1998)

mounted on the ground to drive three pantograph mechanisms. There are three spherical joints between the top of the pantograph mechanisms and the connecting bars, and three revolute joints between the connecting bars and a mobile joystick handle as cited in [24]. The proposed design has a wider workspace and allows for rearrangement of links for increased versatility.

Tsumaki et al. (1998) proposed a design consisting of stick capable of rotating on a 2-DOF spherical manipulator, referred to as a novel five bar spatial Gimbal mechanism for orientation, which in turn is mounted onto a modified delta manipulator. Therefore, the mechanism itself is 6-DOF. The core ideas that the authors wished to implement were the ability to realize quick motion and to have a large workspace while the mechanism itself would be compact.

2.2. Balanced Mechanisms

Balancing can broadly be classified into Shaking Force/Moment balancing and Gravity compensation. Shaking force balancing are created in fast moving machinery in which the centre of mass fluctuates due to the motion of the mechanism. This generates vibrations which are undesirable as they reduce link and joint life. These shaking forces may be due to externally applied forces or due to inertial forces. On the other hand, Gravity compensation counteracts the effects of gravity on the linkages by virtue of the weight of the mechanism. As quoted by Antao et al. (2016) For both position and orientation sensing mechanisms or manipulators, it is important for the mechanism to be balanced because if the user lets go of the mechanism, it would return to its most stable configuration under the action of gravity. Therefore, the

gravity balancing of mechanisms is desired such that their configuration does not change after the last use and according to Millman et al. (1991) Mechanisms should be statically counterbalanced to avoid operator fatigue.

To achieving Balancing, the methods used can be classified into active balancing and passive balancing. As cited by Antao et al. (2016) Active balancing makes use of external actuators which may be electric, hydraulic or pneumatic in nature. Examples of this are given by Arakelian (2016) in which continuous gravity compensation is achieved by the pumping of fluid from the first reservoir (counterweight) to the second.

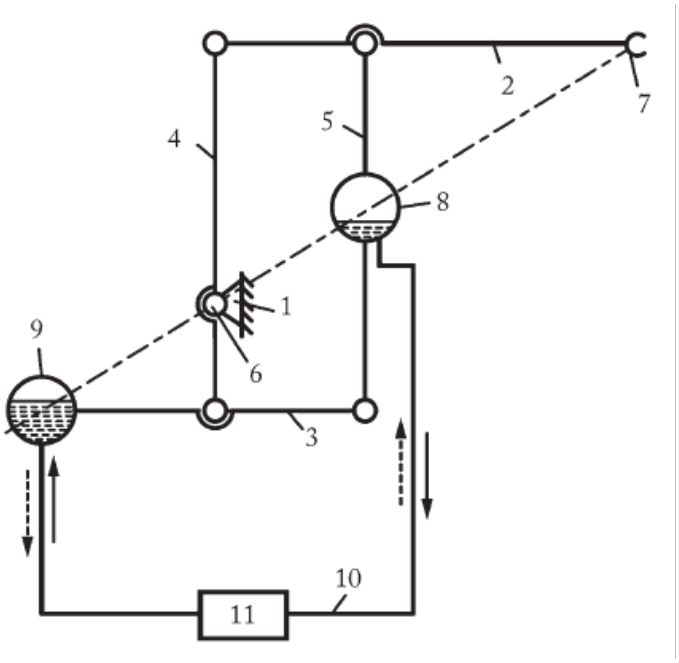

Fig (2.7) Active balancing by pumping fluid from the first reservoir to the second (Arakelian, 2016)

As mentioned by Zhang et al. (2015) Passive balancing, also utilizes compensation inertia or springs. Since the external actuators are not required in passive balancing, it is more economical, simple and energy efficient compared to active balancing. These methods are also more versatile and allows for a significant reduction of the weight of the system as compared to active methods.

According to Gosselin (2008), Mechanisms are said to be force-balanced when the total force applied by the mechanism on the fixed base is constant for any motion of the mechanism. In other words, a mechanism is force-balanced when its global centre of mass remains stationary (fixed), for any arbitrary motion of the mechanism. This condition is very important in machinery since unbalanced forces on the base lead to

vibrations, wear and other undesirable side effects. A mechanism is said to be statically balanced when the total weight of the link does not produce any torque on the joints under static conditions, for any configuration of the mechanism. A mechanism is said to be reactionless or dynamically balanced if, for any motion of the mechanism, there is no reaction force (excluding gravity) and moment on its base at all times as defined by Gosselin (2008) i.e. in addition to being force-balanced, the mechanism should also have a constant angular moment. It should also be understood that dynamic balancing is a property of masses in motion and is unrelated to actuation.

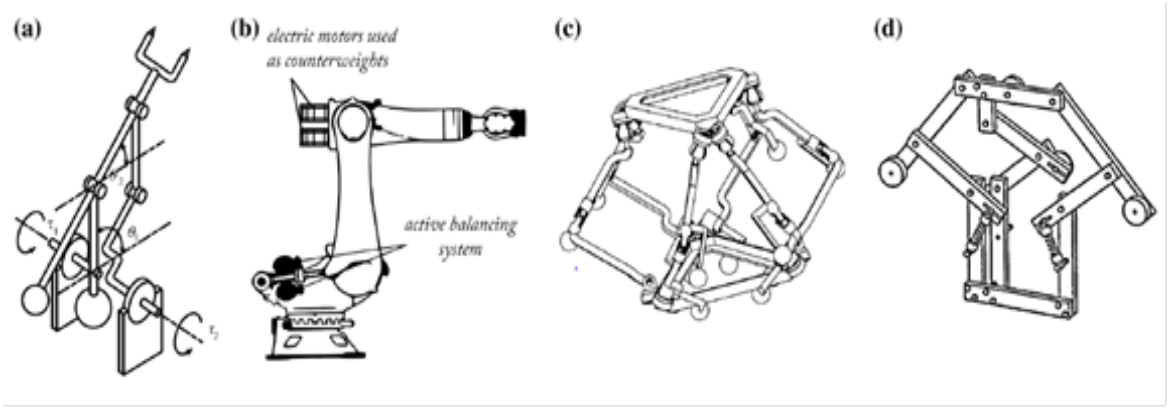

Fig (2.8) Gravity Balancing using counter weights: serial (a,b) and parallel (c,d) manipulator (Arakelian, 2016)

Gravity compensation can be achieved either by using counter masses on the initial system of the mechanism to move the global centre of mass to a stable unchanging position. Sometimes the mass of the system is redistributed to reduce the action of gravity. This is done by planned placement of motors or also through link design and effective material removal which is see in Industrial robots and many such applications. Balancing can also be done using inertia springs and also sometimes using cams and/or pulleys. Gravity compensation through the use of springs can then be defined when the total potential energy in the mechanism including the energy stored in the springs, is constant for any configuration of the mechanism. Springs are normally preferred because they do not add too much mass to the entire system.

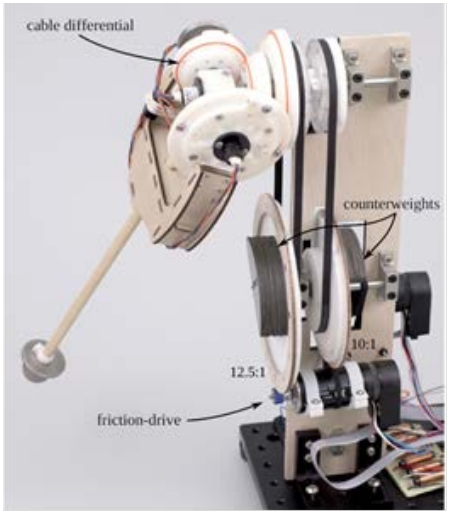

Fig (2.9) Counterweights placed on an Anthropomorphic arm
(Whitney et al. 2014)

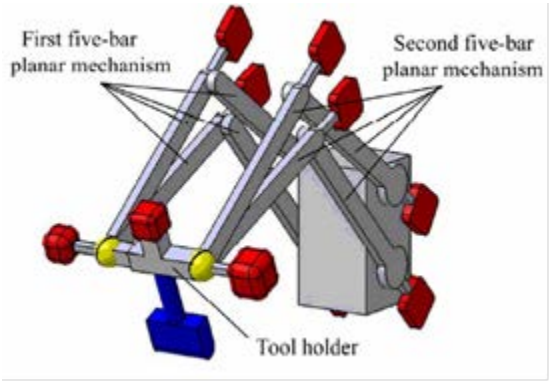

Fig (2.10) Counterweights placed on the manipulator of the Ultrasound Imaging Tool
(Lessard et al. 2007)

Whitney et al. (2014) used gravity counterbalancing techniques to reduce the overall load on the motors, which would otherwise utilize the entire torque available. As inferred by the authors, this allows motors to be sized to the dynamic loads, allowing for faster motion. The issues addressed by them in [24] are that counterweights increase the weight of the system and that the inertia spring systems are mechanically complicated. Lessard et al. (2007) has also used counterweight balancing techniques on the initial system of a parallel robot used in Ultrasound Imaging. This has also contributed to the overall safety of the robot which is a great concern as it is used in close proximity with humans. In this robot, the problem of addition of weight due to counterweights is addressed through implementing methods of partial optimal static balancing which is formulated by the input torques root-mean-square values minimization. Also Briot et al. (2015) has addressed a key issue with gravity compensation i.e. variable weight of the system. This can be done using active counterweights in which the position is modified through the use of extra actuators, but the overall complexity of the system increases. Another technique used is as listed above, in which fluid is pumped between counterweights to allow for continuous gravity balancing. Briot et al. (2015) have proposed a novel energy efficient gravity compensation system for a changing payload through the addition of an adaptive balancing module which incorporates a spring and is tested on the KUKA KR 700PA. In addition to this an extra revolute joint is added to provide the robot with a pantograph linkage to which the adaptive module is connected. No extra energy is

utilized as the energy stored in the spring by virtue of its stiffness is sufficient for a range of variable payloads.

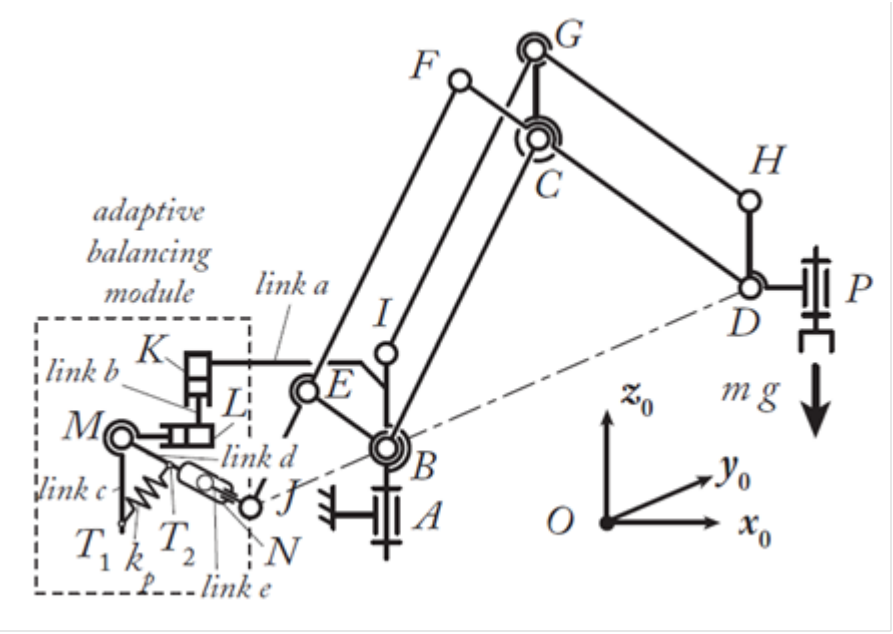

Fig (2.11) KUKA KR 700PA Robot with an adaptive balancing module incorporating a spring
(Briot et al. 2016)

Many other industrial robots also achieve gravity compensation through the use of springs. Azadi et al. (2015) has carried out optimal balancing of a PUMA like robot using inertia springs in order to reduce the energy consumed by the robot and also to reduce the actuator size. Optimal balancing is considered as an integration of control and balancing and is performed in this case due to the predefined path of the robot which enabled the authors to achieve the unknown parameters and trajectory of the system using optimal control, details of which are out of the scope of this project. Gravity balancing can also play a vital role in the development of exoskeletons. Cheng et al. (2015) proposed a design of an exoskeleton, used in rehabilitation applications which is gravity balanced as it offers advantages such as elimination of excess weight due to the presence of motors, which in turn reduces the overall load acting on the patient. It also minimizes the resistance of lifting due to its own weight. The challenge faced in [10] is the variation of torque about each joint due to the orientation and location of each part of the arm. This is solved through a passive method which compensated the torques on each joint.

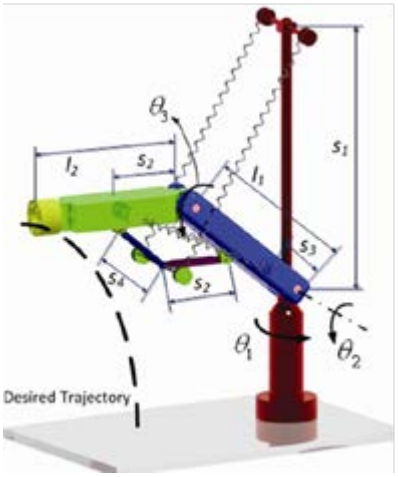

Fig (2.12) PUMA-like robot using spring balancing (Azadi et al. 2015)

2.3. Hand Operated Balanced Manipulators

This term is defined by Arakelian (2004) in [3] as "a handling system with a simple mechanical actuator in which the manipulated object in any position of the workspace is also balanced". This allows for a constant state of gravity cancellation and also a reduction in resistance of the mechanism to be operated by the user. This decreases the overall fatigue felt due to the load acting on the hand. These mechanisms are a low cost, high weight carrying capacity, easy to use and relatively simple to design as compared to using exoskeletons. Hence they are already broadly used in industries to hoist materials or to control heavy machinery/mechanizations, etc.

The procedure for applying gravity compensation of the HOBM depends on the structural design of the manipulator and the type of actuation. The motion of the links, which depend on the type of application will determine the way of carrying out gravity compensation such that the user doesn't work against gravity or against the weight of the mechanism. Hence it is imperative to study the trajectory of the centre of mass of the system as it carries the payload while offering the least possible resistance to the user but at the same time giving the user optimal control. Another example of using a HOBM is explained in [19] which describes the research on linking a robot capable of performing surgery to a surgeon at a remote location. As quoted by Antao et al. (2016) "HOBMs can be used so that the surgeon has a certain familiarity in handling the robot. To further develop this familiarity, dynamic and static balancing enable a finely tuned manipulator to accomplish tasks such that the surgeon feels immersive during the surgery".

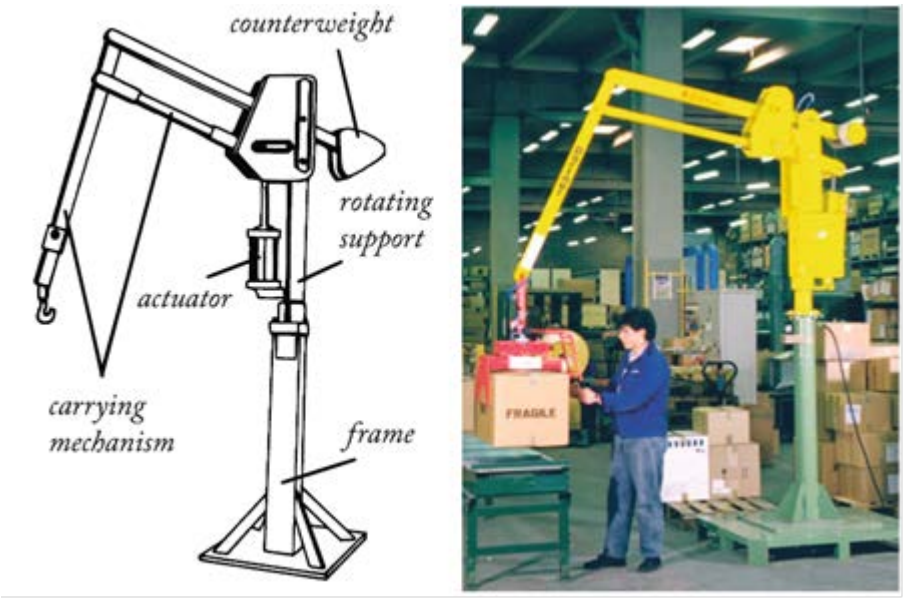

Fig (2.13) Hand Operated Balanced Manipulators (Arakelian et al. 2014)

There are two ways to perform counterweight balancing: The counterweights can either be mounted on the initial system of the mechanism or they can be mounted on the auxiliary linkages connected with the initial system. As mentioned by Arakelian (2016), an auxiliary link is any mechanical structure that is mounted between the balancing element and the initial structure of the manipulator. The former method is generally used in serial robots and planar parallel robots whereas the latter is used in spatial parallel robots and is generally more complex than the former.

2.4. 3-Revolute Orientation Sensing Mechanism (3- ROSM)

There is a need to measure orientation accurately in a variety of applications as discussed above. There are various limitations in current input devices such as high cost, limited workspace, inadaptability, etc. Also the input device should be used with minimum resistance without causing strain on the user's arm, hence the input device should be gravity compensated. Taking all these aspects of an input device into account, Antao et al. (2016) in (3-R Orientation sensing mechanism) have proposed a novel mechanism called the 3-ROSM (as the mechanism has three revolute joints) which has three moving links (Link1, Link2 and Link3) and a fixed link (Link0) connected in series as shown in Fig (2.4). This mechanism is passively balanced about joints Joint1, Joint2 and Joint3 and the joint axes intersect at a central point in order to measure orientation accurately. This emulates the wrist of a 6-axis wrist partitioned robot. The end effector (EE) has a spherical shaped object which can be held by the user to change the configuration of the mechanism. When the user tries to move the EE, the center of the sphere remains at the same position, as the three axes intersect and the only thing that changes is the orientation of the EE, with respect to the fixed link (ground). To simplify the problem of gravity compensation of the 3-ROSM, the novel features proposed are T-shaped extended links which are attached to the initial system. These allow for reduction of a 3 Dimension balancing problem into a 2 Dimension balancing problem, thereby reducing the complexity of the problem. Simulations were performed for dynamic analysis on the mechanism and the results are reported in [1].

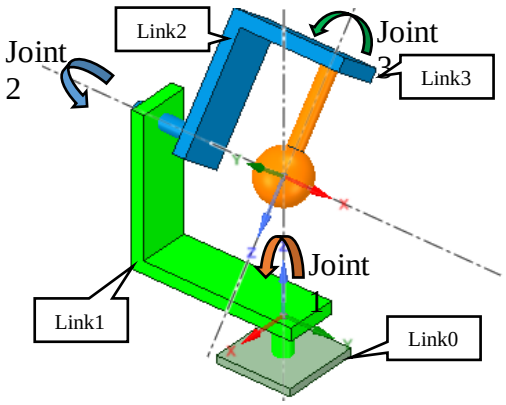

Fig (2.14) CAD Model of 3-ROSM (Antao et al. 2016)

3.Kinematic Analysis

Kinematics studies the motion of bodies without consideration of the forces or moments that cause the motion. Robot kinematics refers to the analytical study of the motion of a robot manipulator. Formulating the suitable kinematics models for a robot mechanism is imperative for analyzing the behavior of industrial manipulators.

3.1. Forward Kinematics and Inverse Kinematics

Forward kinematics is concerned with the relationship between the individual joints of the robot manipulator and the position and orientation of the tool or end-effector. Stated more formally, forward kinematics is used to determine the position and orientation of the end-effector, given the values for the joint variables of the robot. The joint variables are the angles between the links in the case of revolute or rotational joints, and the link extension in the case of prismatic or sliding joints.

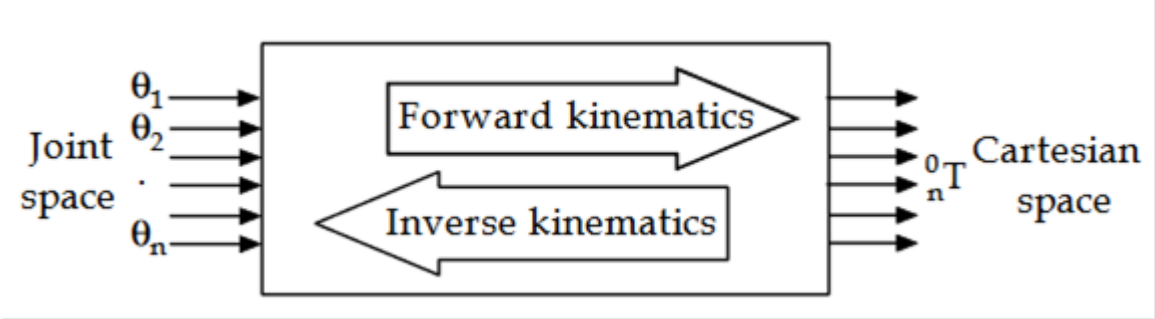

Fig (3.1) Schematic representation of Forward and Inverse Kinematics
(Kucuk et al. 2006)

Inverse kinematics makes use of the kinematics equations to determine the joint parameters that provide a desired position for each of the robot's end-effectors. Specification of the movement of a robot so that its end-effectors achieve the desired tasks is known as motion planning. Inverse kinematics transforms the motion plan into joint actuator trajectories for the robot. Solving the inverse kinematics is computationally expansive and generally takes a very long time in the real time control of manipulators. Tasks to be performed by a manipulator are in the Cartesian space, whereas actuators work in joint space. Cartesian space includes orientation matrix and position vector. However, joint space is represented by joint angles. The conversion of the position and orientation of a manipulator end-effector from Cartesian space to joint space is called as inverse kinematics.

3.2. Denavit Hartenberg Representation

The architecture of the proposed serial mechanism can be represented using the Denavit-Hartenberg (DH) parameters which is a commonly used convention for selecting frames of reference in robotic applications. Four parameters, joint angle, link offset, link twist and link length are used to represent the position and orientation, collectively known as configuration, of the DH coordinate frame attached on a link, with respect to the DH coordinate frame attached on the previous link. A brief explanation of these parameters is given in Table [3.1] and illustrated in Fig (3.2). The nomenclature and methodology described in [17] is followed in this paper, where more details about the procedure on DH parameters assignment can be found. The Text below is adapted from our earlier work in [1].

Parameter	**Description**
Joint offset (b_i)	Distance between X_i and X_{i+1} along Z_i
Joint Angle (θ_i)	Angle between X_i and X_{i+1} about Z_i
Link Length (a_i)	Distance between Z_i and Z_{i+1} along X_{i+1}
Twist Angle (α_i)	Angle between Z_i and Z_{i+1} about X_{i+1}

Table [3.1] Description of DH Parameters

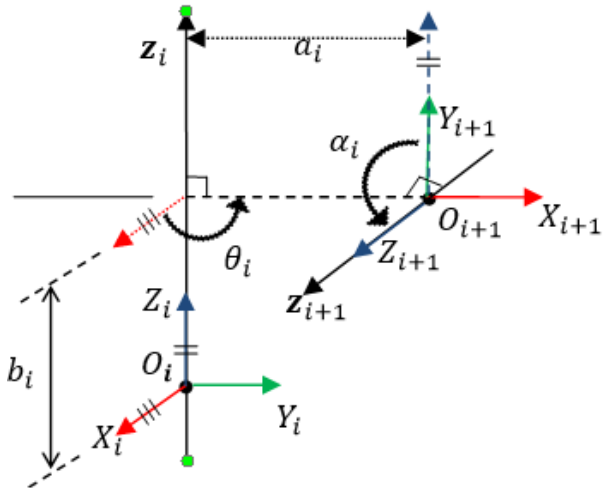

Fig (3.2) DH parameters between frame$_i$ and frame$_{i+1}$ (Antao et al. 2016)

A Homogeneous Transformation Matrix (HTM) is used to represent the configuration between two DH coordinate frames. For example, the HTM between Frame$_{i+1}$ with respect to Frame$_i$ is given by

$$\mathbf{T}_i = \begin{bmatrix} \cos\theta_i & -\sin\theta_i \cos\alpha_i & \sin\theta_i \sin\alpha_i & a_i \cos\theta_i \\ \sin\theta_i & \cos\theta_i \cos\alpha_i & -\cos\theta_i \sin\alpha_i & a_i \sin\theta_i \\ 0 & \sin\alpha_i & \cos\alpha_i & b_i \\ 0 & 0 & 0 & 1 \end{bmatrix} \quad (1)$$

As the position of the EE of 3-ROSM remains invariant, the DH coordinate frame attached to the fixed link (Link0) can be assumed to be at the center of the spherical EE, such that the Z axis, i.e., Z_1, of Frame1 (attached to Link0) is along the direction of the axis of Joint1, as shown in Fig (3.3(a)). The X axis of Frame$_1$, i.e., X_1, can be taken arbitrarily. Y_1 axis is computed as a cross-product between the Z_1 and X_1 axes. As per the DH parameter convention, the DH coordinate frame, Frame$_2$, attached to Link$_1$ has to be located such that Z_2, is along the axis of Joint1. This makes Z_1 and Z_2 collinear and hence the origin of Frame$_2$ (O_2) has to be along Z_2. Though there exist infinite number of points on the axis of Joint1, where O_2 can be located, it is coincided with O_1, to simplify the resulting mathematical expression. X_2 can be chosen arbitrarily such that it is orthogonal to Z_2, and Y_2 can be found using cross-product rule. Of the four DH parameters; joint offset (b_1), link length(a_1) and twist angle (α_1) are all zero. The only variable is joint angle (θ_1) which is the angle between X_2 and X_1, which changes as Joint1 is rotated. The HTM of Frame$_2$ with respect to Frame$_1$ can be determined using the expression given in Fig (3.3(b)).

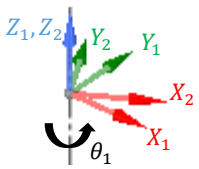

(a) Frame1 and Frame2

$$\mathbf{T}_1 = \begin{bmatrix} \cos\theta_1 & -\sin\theta_1 & 0 & 0 \\ \sin\theta_1 & \cos\theta_1 & 0 & 0 \\ 0 & 0 & 1 & 0 \\ 0 & 0 & 0 & 1 \end{bmatrix}$$

(b) HTM of Frame2 with respect to Frame1

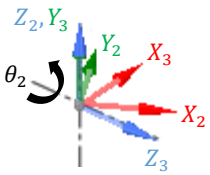

(c) Frame2 and Frame3

$$\mathbf{T}_2 = \begin{bmatrix} \cos\theta_2 & 0 & \sin\theta_2 & 0 \\ \sin\theta_2 & 0 & -\cos\theta_2 & 0 \\ 0 & 1 & 0 & 0 \\ 0 & 0 & 0 & 1 \end{bmatrix}$$

(d) HTM of Frame3 with respect to Frame2

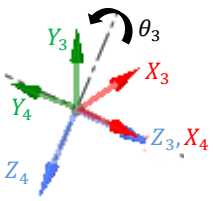

(e) Frame3 and Frame4

$$\mathbf{T}_3 = \begin{bmatrix} \cos\theta_3 & 0 & \sin\theta_3 & 0 \\ \sin\theta_3 & 0 & -\cos\theta_3 & 0 \\ 0 & 1 & 0 & 0 \\ 0 & 0 & 0 & 1 \end{bmatrix}$$

(f) HTM of Frame4 with respect to Frame3

Fig (3.3) DH frames attached to the links of the mechanism (Antao et al. 2016)

Once Frame$_2$ is completely determined, Frame$_3$ (attached on Link2) has to be found. Z_3 has to be along axis of Joint2. Since Z_2 and Z_3 intersect, origin of the frames Frame$_2$ and Frame$_3$ coincide. As X_3 has to be perpendicular to both Z_2 and Z_3, it can be obtained as $Z_2 \times Z_3$ (though $Z_3 \times Z_2$ can also be taken). Y_3 can be obtained using

cross-product rule. Of the four parameters between frames $Frame_2$ and $Frame_3$, joint offset (b_2) and link length (a_2) are zero due to intersecting joint axes. The joint angle (θ_2) is a variable, i.e., the angle between X_2 and X_3, which changes when Joint2 is rotated. The fourth parameter, twist angle (α_2) is 90°, since Z_2 and Z_3 intersect orthogonally, due to the virtue of the construction of the mechanism. $Frame_2$ and $Frame_3$ are illustrated in Fig (3.3(c)) the corresponding HTM is given in Fig (3.3(d)). Similarly, Joint2 and Joint3 intersect as shown in Fig (3.3(e)) and the HTM is given in Fig (3.3(f)). The DH parameters for the entire mechanism is given in Table [3.2].

Parameter / Joint	Joint offset (b_i)	Joint Angle (θ_i)	Link Length (a_i)	Twist Angle (α_i)
Joint1	0	θ_1 (variable)	0	0°
Joint2	0	θ_2 (variable)	0	90°
Joint3	0	θ_3 (variable)	0	90°

Table [3.2] DH Parameters of the 3-R Orientation Sensing Mechanism

The HTM of $Frame_4$ with respect to $Frame_1$ is determined by multiplying the individual HTMs as

$$\mathbf{T} = \mathbf{T}_1\mathbf{T}_2\mathbf{T}_3$$

$$= \begin{bmatrix} \cos(\theta_1+\theta_2)\cos\theta_3 & \sin(\theta_1+\theta_2) & \cos(\theta_1+\theta_2)\sin\theta_3 & 0 \\ \sin(\theta_1+\theta_2)\cos\theta_3 & -\cos(\theta_1-\theta_2) & \sin(\theta_1-\theta_2)\sin\theta_3 & 0 \\ \sin\theta_3 & 0 & -\cos\theta_3 & 0 \\ 0 & 0 & 0 & 1 \end{bmatrix} \quad (\mathbf{2})$$

This HTM has two primary components. The elements in the first three rows and three columns correspond to the orientation between $Frame_4$ and $Frame_1$, representing the direction-cosines. These elements are a function of joint angles of Joint1, Joint2 and Joint3. The elements in the fourth column and first three rows correspond to the position of the origin of $Frame_4$ with respect to that of $Frame_1$. Note that all the elements are zero and are independent of the joint angles. Hence, the proposed mechanism can be used as an Orientation Sensing Mechanism.

4.Design of the 3-ROSM

It is now found out that the 3-ROSM can be used as an orientation sensing device, but as it is currently if the user lets go of the end effector, the mechanism will reorient itself into its most stable configuration due to the action of gravity. As mentioned in Chapter 2.2, passive balancing, namely gravity compensation using counterweights is preferred due to their simplicity and low cost. Hence, there is a need to modify the design of the 3-ROSM such that it can accommodate the counterweights without affecting the overall working of the mechanism.

4.1. Modification of Links

In the proposed mechanism, gravity compensation is achieved by placing counterweights on modified T-shaped extensions which are attached to Joint 1 and Joint 2 have opposite shapes to the original shapes of Link1 and Link2 respectively, of the 3-ROSM. It should be duly noted that link 3 possesses a spherical end effector grip and is symmetric about the axis of Joint3 and is thus balanced. For the purpose of further balancing of the entire mechanism, the CG of Link3 will be considered as an extra mass added on Link2 and the relative position of the CG of Link3 with respect to Link2 remains constant. Also, the extended links have their CG away from the axes of their respective Joints.

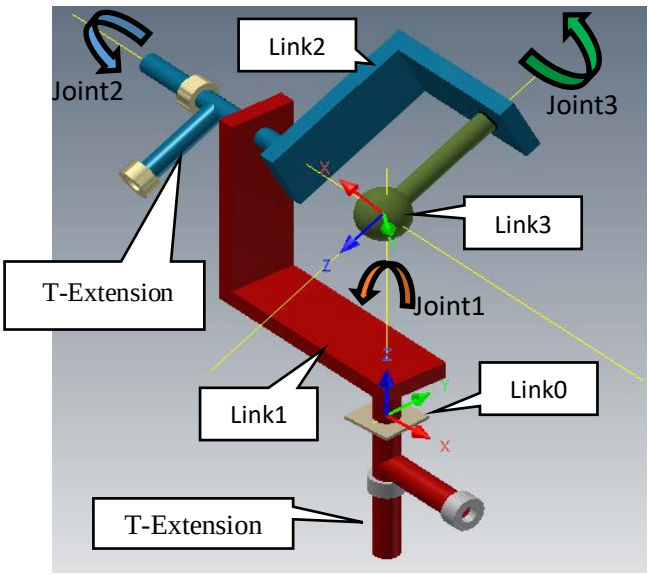

Fig (4.1) CAD model of the 3-ROSM with extensions (Antao et al. 2016)

The novelty of the T-shaped extensions is that the balancing problem which existed in 3 Dimensions is now reduced to two 2 Dimension balancing problems which are relatively simple to solve and implement. This is because the extensions give two orthogonal directions to adjust the placement of counterweights. If the balancing is disturbed due to the passage of time or with addition of extra masses on the links, the counterweights can be moved along the orthogonal extensions to compensate the changes.

The end result achieved is that the combined CG of all the Links and counterweights lie along the axis of Joint1 and hence is balanced for any θ_1 rotation. Therefore, not only does the mechanism retain its shape for any action of gravity or its components, but with the decrease of friction acting on the joints, the mechanism itself becomes smooth, easy to use and offers least possible resistance to the user's arm which reduces fatigue.

4.2 Balancing of Link2 and Link3 about Joint2 axis

Consider Fig (4.2(a)), consider the masses of Link3 as m_3 and of Link2 as m_2. Let the counterweights be cm_{2z} along the Z axis (axis of Joint2) and cm_{2x} along the X axis (transverse direction). Different length parameters used for calculations are as shown in the Figure. (The following work was done using Autodesk Inventor and its Dynamic Simulation Module; practical validations were reported in our previous work [1].)

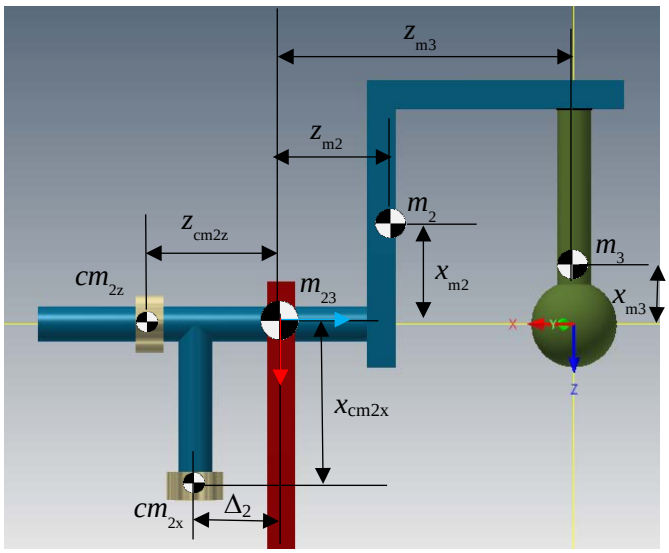

(a) Link2 and Link3

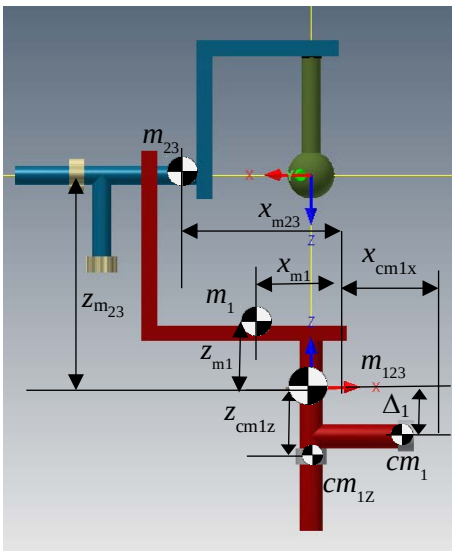

(b) All links

Fig (4.2) Balancing of the 3-ROSM using counterweights (Antao et al. 2016)

It is desired that the effective CG of the two links, with extensions and the counterweights coincide at the support point for Joint2 on Link1, represented using m_{23}. This is achieved by equating the moments about the *Z* and *X* axes, respectively, as

$$(m_2 \cdot x_{m2}) + (m_3 \cdot x_{m3}) = (cm_{2x} \cdot x_{Cm2x}) \quad (3)$$

$$(m_2 \cdot z_{m2}) + (m_3 \cdot z_{m3}) = (cm_{2z} \cdot z_{Cm2z}) + (cm_{2x} \cdot \Delta_2) \quad (4)$$

The primary principle used in the counterweight balancing of the 3-ROSM is that the mass of the counterweights is fixed and only the distances are varied. From Equations (3) and (4), the distances cm_{2x} and cm_{2z} can be determined.

4.3. Balancing of all Links Along Joint1 Axis

Since the combined mass of Link2, Link3, cm_{2x} and cm_{2z} is invariant in the plane containing axes of Joint1 and Joint3. These masses can be replaced by mass m_{23} on Joint2, as shown in Fig (4.2(b)). For the gravity balancing along Joint1 axis, the combined mass of m_{23} and m_1 are balanced by counter masses cm_{1x} and cm_{1z} placed on the sliders on Link1, such that the combined mass of all the links and counter masses (m_{123}) is on axis of Joint1. The coordinates x_{cm1} and z_{cm1} for the placement of counter masses can be obtained using

$$(m_{23} \cdot x_{m23}) + (m_1 \cdot x_{m1}) = (cm_{1x} \cdot x_{Cm1x}) \quad (5)$$

$$(m_{23} \cdot z_{m23}) + (m_1 \cdot z_{m1}) = (cm_{1z} \cdot z_{Cm1z}) + (cm_{1x} \cdot \Delta_1) \quad (6)$$

Hence by using the countering the moment acting on the links due to gravity through the use of counterweights, the design of the 3-ROSM successfully withstood the effect of gravity and its components acting on it. The next stage of design would implement the practical development of the 3-ROSM and to tackle real challenges such as friction, retrieving data such as joint angles from the device and also to address the issue of the device having a point of singularity when the axes of Joint1 and Joint3 are align.

5.Prototype I

The primary task of developing Prototype I was to validate the theory of the 3-ROSM, not only the counterweight balancing techniques performed, but also its usability as an orientation sensing mechanism i.e. If the friction in the joints is high, then it will be difficult to measure joint angles as there will always be backlash of values. It would also be tough to validate the counterweight balancing techniques, due to the fast that the low values of moment acting on the model are heavily influenced due to friction.

5.1. Fabrication of Prototype I

It was decided that Links of the prototype would be developed using acrylic with the dimensions obtained from the CAD model. Acrylic has good rigidity and is easy to work and relatively less expensive as compare to a full metal model. The shafts were constructed from aluminium rods which are light weight allowing for the majority of the weight to be distributed on the links.

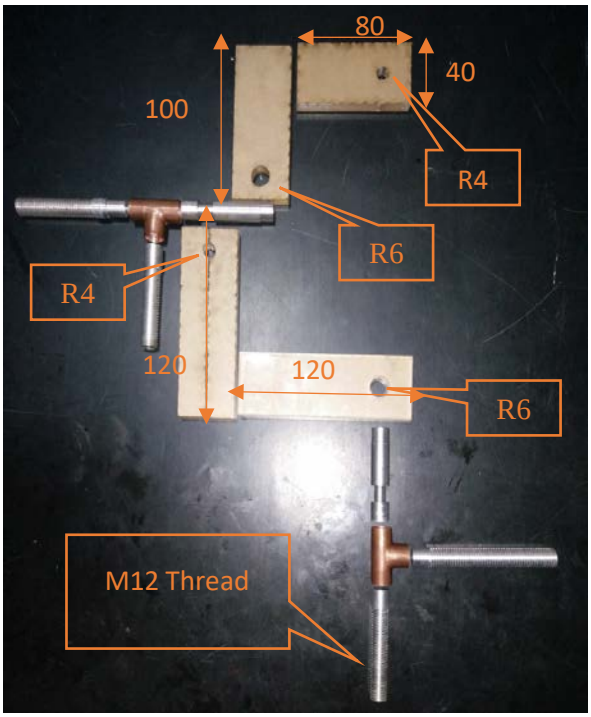

Fig (5.1) Parts of Prototype I (All Dimensions in mm)

The links were subjected to laser cutting, which is done by designing the parts in AutoCAD and exporting them as a .PDF file which is then inputted into the laser printer so that the precise location of the cut is known. It should be noted that while designing thickness of the laser should be considered to get proper dimensions (In this

case the laser thickness was 1mm). The aluminium rods were subjected to turning and facing operations in a lathe machine to get precise parts. The aluminium rods were then threaded on the lathe machine with a M12 thread x 1.75 pitch. The idea was to design threaded T-shaped extensions to allow for better resolution and also so that the balancing can easily be changed if there is any change is the mass of the system. This is another novel feature of the 3-ROSM. In order to make these extensions copper T connectors were purchased to allow for uniformity of the extensions. This is done so that the production of this prototype in future would be faster as the parts are readily available in the market. Another challenge faced was the fabrication of revolute joints with minimum friction and also to reduce play in these joints such that they only revolve and do not translate about any other axis. The first revolute joint was made using a 10mm ball bearing at Joint1. This is done because the load acting on Joint 1 is the highest and only a bearing is capable of reducing the friction while at the same time dissipate the load without hampering the revolution of Joint1. The procedure taken for Joint 2 was different; the vertical portion of Link1 was split into two and rejoined over Joint 2 which had a smaller diameter than the rest of the shaft. This eliminated translation motion about any other axis. The same procedure is applied to Joint3 but the addition of grub screws was necessary to keep Link3 in place and to prevent it from falling due to gravity. Finally, the entire device is assembled and tested for gravity compensation.

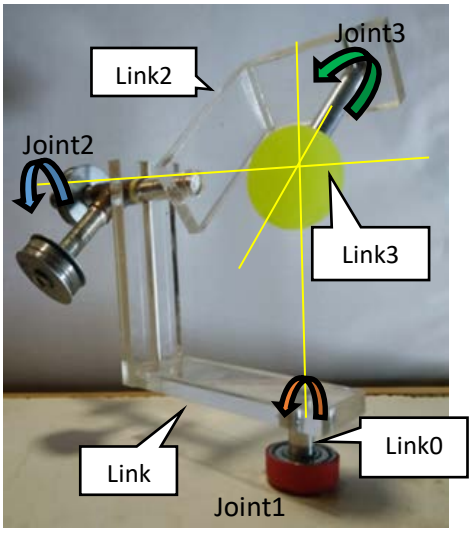

Fig (5.2) Prototype of the 3-ROSM

The center of gravity (CG) of the links, which are a combination of primitive shapes, can be found theoretically using the size and density of the material of the links. But due to the fact that no material can have uniform density, which can be caused by manufacturing defects or during machining processes, it is required to find a practical CG as well in order for the balancing to be accurate.

5.2. Hanging Method

It is a commonly known method to find the practical CG value of an object no matter how complex the object may be. The CG may lie on the object or it may lie off-plane, which may be due to high mass distribution. The procedure for each experiment involves hanging the link under consideration by different points from a fixture and dropping a vertical plumb line from the same fixture. The string holding up the link is considered massless as its weight is negligible as compared to the link itself. It is known that the CG always lies below the point of suspension. Therefore, the intersection of two plumb lines for different orientations of the link is taken as its CG. However, a third plumb line is also drawn for a different link orientation to validate the intersection point. In the case of the T-shaped extensions the CG lay on the extension itself, but with all the links, due to the presence of high mass concentrations distributed on the link, the CG was off-plane. Hence to measure these CG values, a paper (considered massless) is attached to the link. Hence, when it is hung the point can be located on the paper. The plumb line and thread by which the link is hung, should be in line and parallax must be avoided to produce an accurate result.

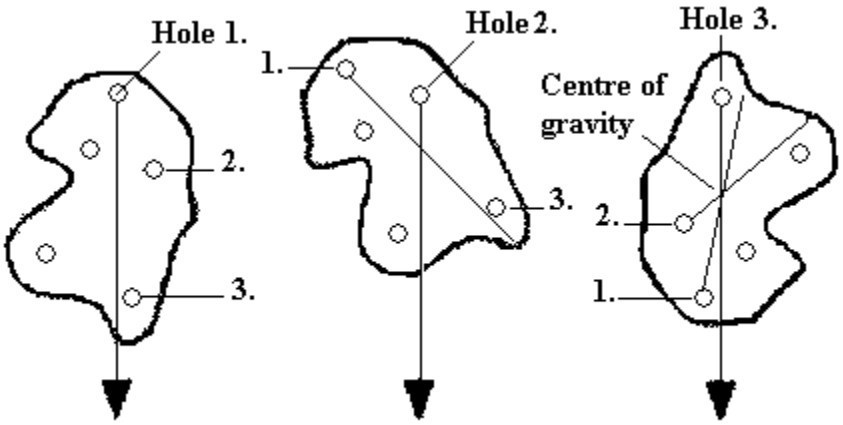

Fig (5.3) Schematic representation of the Hanging method
(Source: Google)

5.3. Images, Tabulations and Results

(a) (b) (c)

Fig (5.4) Hanging method performed on T-shaped Extension 1

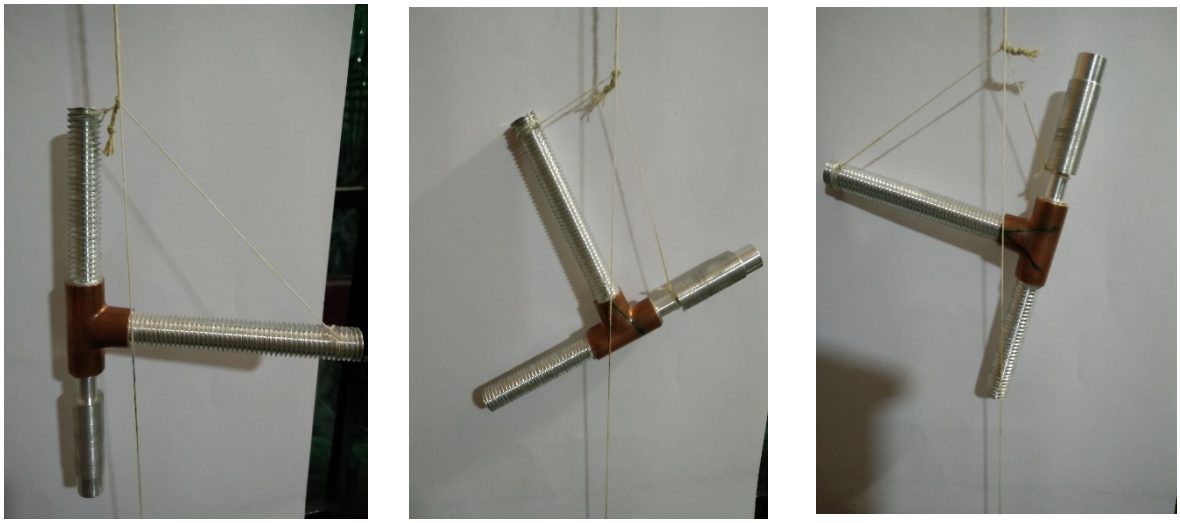

(a) (b) (c)

Fig (5.5) Hanging method performed on T-shaped Extension 2

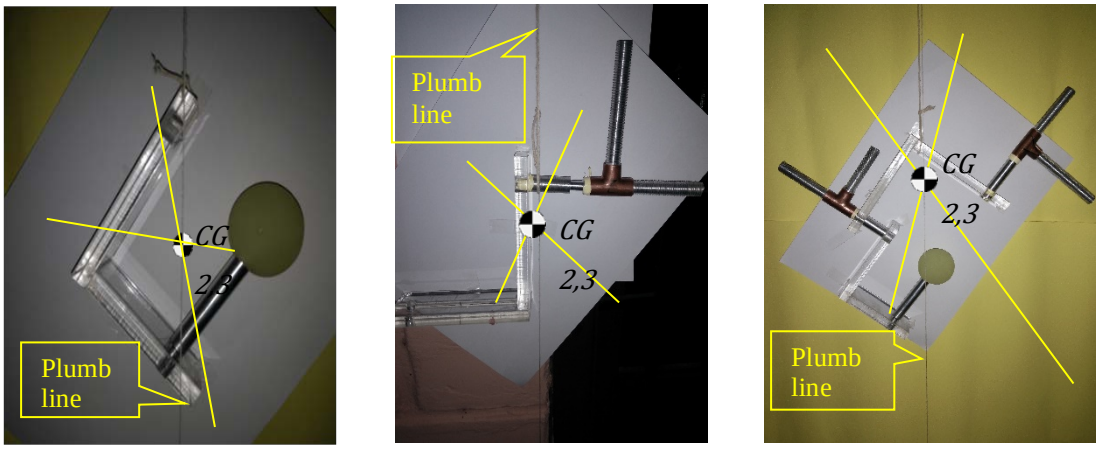

(a) (b) (c)

Fig (5.6) Hanging method performed on Link configurations of the 3-ROSM

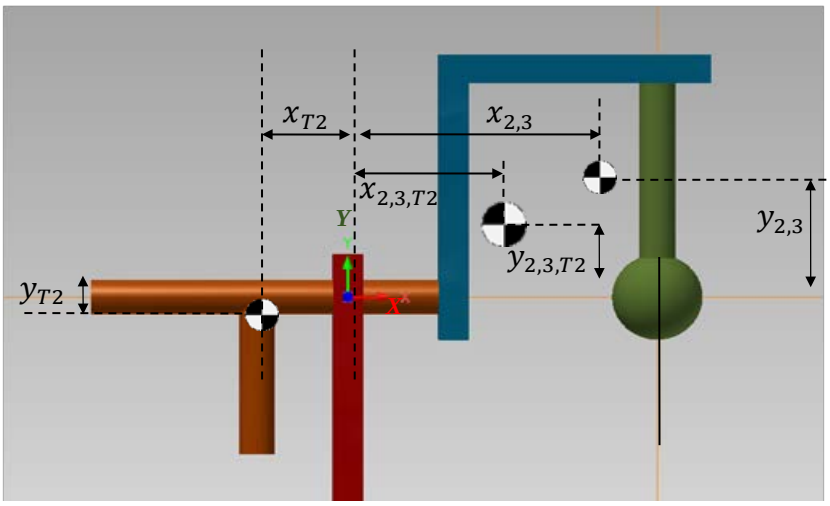

Fig (5.7) Center of Gravity (CG) of links to find locations of counterweights about Joint2 axis

In addition to this, the values of the theoretical CG and the CG values found from the hanging method were tabulated in Table [5.1] and Table [5.2], and the variation between the two shows that even a difference of 2 mm causes a lot of variation in the counterweight position. The thickness of the weights must be kept in mind so that it does not become a distributed mass, thereby contradicting consideration of the counterweights as point masses. Another result that can be derived from the prototype is that the threaded portion possesses infinite resolution for the accommodation of the counterweights, which is also a novel feature of this mechanism.

	Link	Mass (g)	Location of CG value using Theoretical Formula (mm)		Location of CG value using Hanging Method (mm)	
			X	Y	X	Y
1.	T-Extension on Link2 (T2)	68.74	-27.26	-11.94	-27.50	-9.20
2.	Link2 and Link3 (2,3)	137.21	68.43	41.60	68.50	39.40
3.	Link 2 and Link 3 with T-Extension 1 (2,3,T2)	205.95	36.49	27.33	36.50	29.10

Table [5.1] CG locations for Joint2 Balancing with Local Coordinate Frame (on Link1)

The CG locations shown in Table [5.2] are with respect to a global coordinate frame located on the axis of Joint1 where the moment of the prototype is balanced. Nomenclature for the same in shown in Fig (5.8).

Sl.No	Link	Mass (g)	Location of CG value using Theoretical Formula (mm)		Location of CG value using Hanging Method (mm)	
			X	Y	X	Y
1.	T-Extension 1	74.53	15.14	-33.22	16.00	-31.00
2.	T-Extension 2	68.74	-129.76	118.06	-129.50	120.80
3.	Link 2 and Link 3	137.21	34.07	171.60	34.00	169.40
4.	Link 2 and Link 3 with T-Extension 2	205.95	66.01	157.33	66.00	159.10
5.	Link 1 with T-Extension 1	183.10	-35.09	19.24	-34.00	20.40
6.	Link 1, Link 2 and Link 3 with T-Extension 1 and T-Extension 2	389.05	-51.37	89.33	-51.50	90.50

Table [5.2] CG locations for Joint1 balancing with Global Coordinate Frame

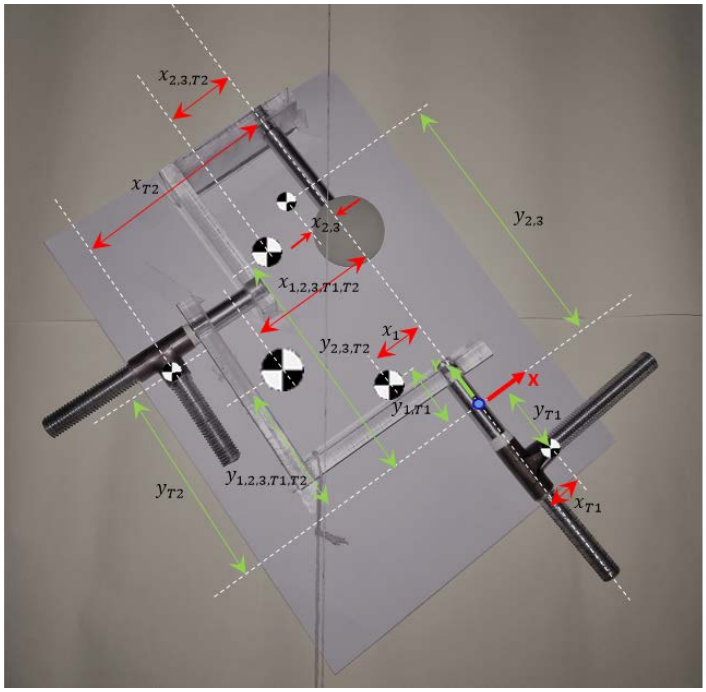

Fig (5.8) CG of links to find location of counterweights about Joint1 axis

Finally, the 3-ROSM Prototype I is assembled together and the counterweights, which are taken as 62g and 65g for Link2 and Link3 about Joint2 axis, are placed to achieve passive balancing of the entire mechanism. There is an existence of a small amount of friction, but the motion of the mechanism is relatively smooth.

(a) (b)

Fig (5.9) Different configurations of the passively balanced 3-ROSM

(c)

(d)

Fig (5.9) Different configurations of the passively balanced 3-ROSM

Through the development of Prototype I, challenges such as reducing friction in joints and fabrication of a revolute joint without any play were faced. Also it is observed that the counterweight balancing techniques used indeed reduced the load on the user's wrist and increased the smoothness of the control of the prototype. Prototype I is also a low cost model, but does contain a factor of friction which the authors find acceptable and this Prototype does not solve the problem of a singularity formed when the axis of Joint1 merges with Joint2. Since this prototype was fabricated with the dimensions of the CAD model, suitable encoders were not available which could match the shaft size of the prototype. Hence in order to measure the change in joint angles, there is a need to fabricate a second prototype, one which can facilitate the available encoders and can be tested in an application to demonstrate the usability of the 3-ROSM.

6.Prototype II

As explained above, the need for the fabrication of a second prototype arose to facilitate the use of encoders which could then measure and record the change in orientation so that it may be used in an application which demonstrated the usability of the 3-ROSM. To show this, it was decided that the second prototype would attempt to control a 3-axis camera mount in which there would be a 1:1 mapping of the change in joint angle. This is done by modelling a custom 3 axis camera mount which would have three intersecting axes, emulating the 3-ROSM. The encoder itself is very small in size (4mm diameter with a double D cut) and therefore, the entire 3-ROSM has to be scaled down. This is another advantage of the 3-ROSM as the working principle behind it does not matter on the overall size of the mechanism, but can be used on any scale. The challenge faced in Prototype II is the overall light weight of the model and the manufacturing of a number of small intricate parts.

6.1. Fabrication of Prototype II

In this attempt to fabricate a second prototype, for the sake of accuracy the parts are 3D printed so that they would have a near uniform mass density and mass distribution while having accurate dimensions as well. It was felt that the threaded portions of the extensions could be fabricated easily and more accurately using 3D printing which would then have a greater resolution as compared to Prototype I. Another change in the design approach was to try and construct the 3-ROSM which could then be easily assembled and disassembled as and when the user desired. Therefore, in Prototype II there are connectors between Links which facilitate the encoders, which have a double D-cut and these connectors also facilitate smooth rotation between links. Also the counterweights would be mounted on a sleeve which would be 3D printed to ensure good transition over the threaded portion. Hence, the core design ideas incorporated in Prototype II are: To build an easy to assemble model; the connectors used to do this should have special double D slots to accommodate the encoders; and a custom thread should be designed on the shaft in order to have the greatest possible resolution, but at the same time should not be too intricate that it cannot be 3D printed. As in Prototype I, the base is mounted on a bearing.

The changes in design were done to the 3-ROSM and Prototype II was designed in Solidworks 2016. The files for each individual part which are originally in a

.SLDPRT format should be exported as a .STL format so that the details of the part can be read by a 3D Printer. While exporting the file, the units are set to be in millimeters by default, with a custom resolution and the measurement system used is the Binary system and not the ASCII system. While designing, allowances should be given between the mating parts and between rotating parts. Also allowances should be given to the threaded counterweight sleeve such that is does not get stuck while turning over the thread. The thread itself was designed by extruding a swept boss/base profile of the thread over a helical path with the same pitch as the threaded portion. The tips of the thread are filleted to allow for a better quality 3D print.

The designs were then uploaded to a website called 3DHub which has a database of all 3D printing vendors in Bangalore. The website calculates the volume of the part, while checking for intricate details, etc. and then provides three methods by which the part can be 3D printed, namely FDM (Fused Deposit Modelling), SLA (StereoLithography)and SLS (Selective Laser Sintering). Of the three methods the most economical is FDM which has a dimensional accuracy of 0.5mm with the minimum feature detail as 1mm. FDM is an example of an additive manufacturing technique in which the material, in the form of a filament or metal wire is laid down in layers to form the part. The material used can either be PLA (Poly Lactic Acid), ABS (Acrylonitrile Butadiene Styrene) or Nylon. PLA is more rigid and brittle as compared to ABS while Nylon is the most expensive material to use among the three. Since in the fabrication of an orientation sensing mechanism, rigidity of the links is an important factor, therefore PLA is selected as the material for the parts. The next option that the client can choose from is the layer height. The layer height is the height after which the next layer is laid down. This varies from 300 microns to 50 microns and is also dependent on the size of the nozzle which lays down the wires. In a 300 micron 3D print the layers are visible in the form of lines running along the profile of the part whereas a 50 micron layer height allows for more intricate details of the part to be manufactured. In Prototype II a 50 micron layer height is selected to obtain a better quality of parts.

Although FDM is an affordable 3D printing solution, it has limited dimensional accuracy for small parts and both SLS and SLA provide good mechanical properties while allowing for fine feature details. However, since the cost grows exponentially

with the use of SLS and SLA, due to a limited budget it was decided to try and design the parts so that FDM could be used to produce them.

After choosing FDM as the preferred method with PLA as the material, next a vendor (Hub) should be selected with whom the designs are shared. The hub evaluates the feasibility of the 3D print and reviews the designs allowing for correspondence on any beneficial changes that should be implemented. Once the designs are carefully reviewed and no problems are found then the hub demands an upfront payment which goes to the website and upon completion of the task, is then transferred to the vendor. 3DHub offers two modes of delivery: either the parts can be picked up in person or they can be delivered using a courier service.

6.2. Centre of Gravity Calculations

As the Hanging method proved to be a useful technique in determining the CG locations in Prototype I, it finds its use in calculating CG locations in Prototype II as well. Although, this 3D printed version of the 3-ROSM, which weighs a total of 34.914g (counterweights NA) has a more uniform mass distribution than Prototype I, the presence of the encoders mounted on the links makes it difficult to find the CG locations using theoretical methods. In a similar way as shown in sections 5.2 and 5.3, the CG locations are located and using the moment balancing equations, the locations of the counterweights are determined.

(a) (b)

Fig (6.1) Hanging method performed on Link2 and Link3

(a) (b) (c)

Fig (6.2) Hanging method performed on Link2 and Link3 with T-extensions

(a) (b) (c)

Fig (6.3) Hanging method performed on Link1 with T-extensions

As shown above, the finding of the CG location is done with the encoders mounted on the links. The encoders are placed such that they are also symmetric about the same plane as the links of the 3-ROSM. As mentioned previously the axis of the plumb should coincide with the axis of the string by which the links are hung to avoid a parallax error which if ignored produces a significant change in the locations of the CG. The authors acknowledge the fact that the weight of the wires attached to the prototype have not been considered yet.

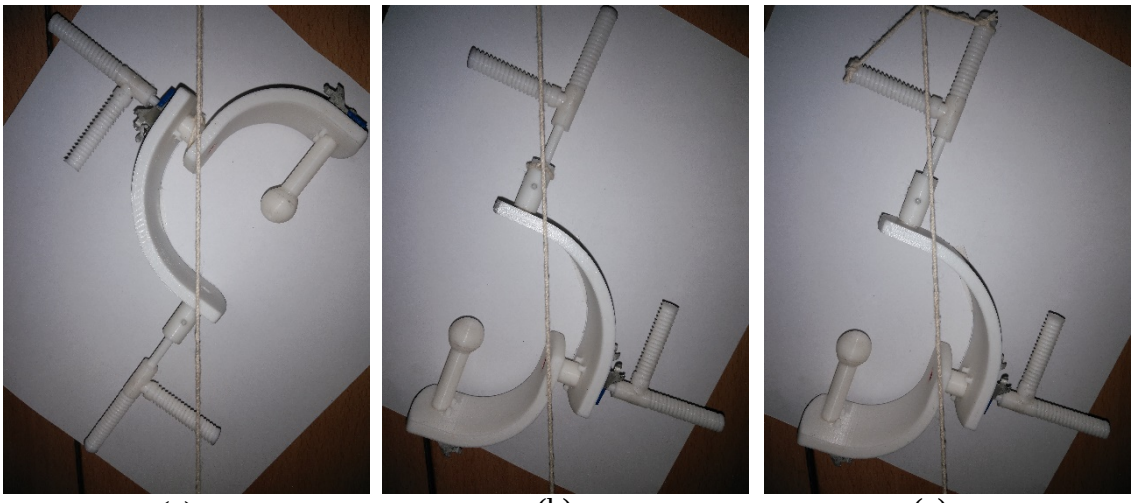

(a) (b) (c)

Fig (6.4) Hanging method performed on the entire 3-ROSM (Prototype II)

This will have an important effect on the overall balancing of the mechanism as the current Prototype II is small and very light due to 3D printed parts. In order to account for these changes, the excess mass will be considered and the counterweights will be adjusted along the threaded extensions to achieve full passive balance of the model. Finally, the entire 3-ROSM (Prototype II) is mounted on the bearing which behaves as Link0 (ground).

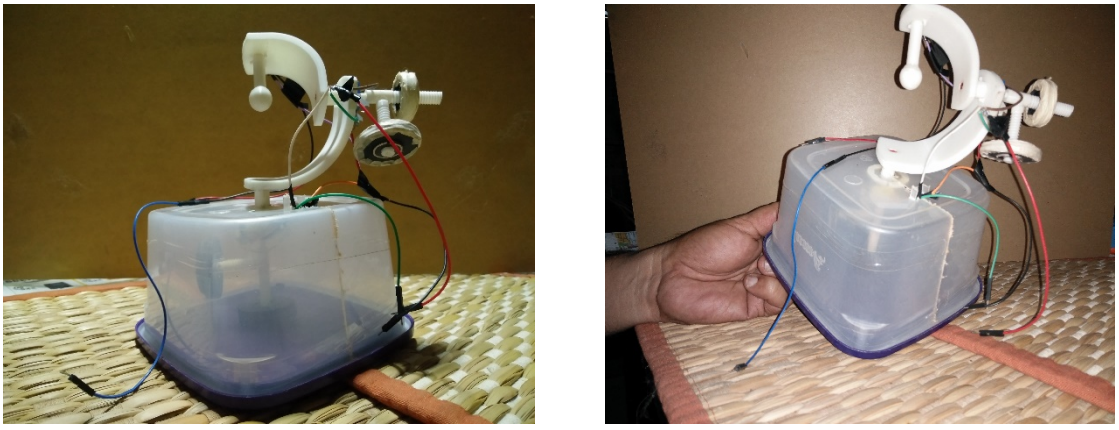

(a) (b)

Fig (6.5) Passively balanced Prototype II using counterweights

7.System Integration

Once the 3 revolute orientation sensing mechanism (3-ROSM) is ready there are two other important objectives to be achieved in the project. The first is to extract the orientation angle values from the 3-ROSM.This is intended to be achieved by integrating hollow bore encoders in to the system interfacing it with an Arduino Uno microcontroller. The second objective is to demonstrate an application of the 3-ROSM. Out of the many applications possible, it was decided to fabricate a Pan-Tilt-Roll camera mount which is to be controlled by the 3-ROSM. Here the first objective is tackled, i.e., to extract the orientation values from the input mechanism.

7.1 Component Description

Components Used	Quantity
Hollow core Encoders	3
Arduino Uno	1
Jumper wires	11

Table [7.1.] Component table

Fig (7.1) Hollow bore encoders (TE connectivity / citec 5350500107 Source: www.element14.com)

The hollow bore encoder is a type of rotary encoder without a knob or horn attached. It has a through hole through which the shaft whose speed is to be measured is inserted. The encoder being used is a TE connectivity 535 series 10 K ohm linear potentiometer with 300 degrees of designed angle of rotation.

A Rotary encoder is an electro-mechanical device that converts the angular position or motion of a shaft or axle to a numerical Rotary value depending on the rotation of

a part called wiper. In this project a 10-bit hollow rotary encoder has been used to extract the angular information. Thus it produces values from 2^0 - 2^10 or 0-1023.

There are mainly two types of encoders; Absolute encoders and relative (or incremental) encoders. The first type of encoders, i.e. Absolute encoders directly point out the angular position and thus the current angle that the encoder is at. Thus they are angle transducers. Relative encoders, on the other hand, provides information about the motion of the shaft, which is typically further processed elsewhere into information such as speed, distance and position.

Rotary encoders are used in many applications that require precise shaft unlimited rotation including industrial controls, robotics, Computer input devices.

The rotary encoders are essentially variable resistors (potentiometers) or voltage dividers. It is a passive linear circuit that produces an output voltage (V_{out}) that is a fraction of its input voltage (V_{in}). Voltage division is the result of distributing the input voltage among the components of the divider. A simple example of a voltage divider is two resistors connected in series, with the input voltage applied across the resistor pair and the output voltage emerging from the connection between them.

The working of a potentiometer is governed by Ohm's law. Ohm's law states that the current through a conductor between two points is directly proportional to the voltage across the two points. Introducing the constant of proportionality, the resistance, the mathematical equation that describes this relationship:

$$V=I*R$$

Where

I, is the current through the conductor in units of Amperes

V, is the voltage measured across the conductor in units of Volts

R, is the resistance of the conductor in units of ohms.

As per the above equation, As Resistance increases, the Voltage drop increases

The resistance of a conductor is given by

$$R=p*L/A$$

R, is the Resistance, **p,** is the resistivity of the conductor

L, is the length of the conductor and **A,** is the Cross section area of conduction

As per the above equation, as the length of conductor increases, the resistance too increases proportionally**.** The above two conclusions essentially mean that as the length of conductor increases the voltage drop changes proportionally. Thus the voltage can be controlled by changing the length of current flow. This is implemented in a voltage divider circuit (or a potentiometer).

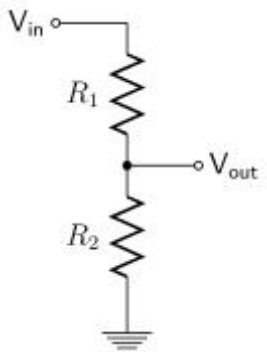

Fig (7.2) Voltage divider circuit (Source: Google images)

$$\mathbf{V}_{out} = ((\mathbf{R2})/(\mathbf{R1}+\mathbf{R2})) * \mathbf{V}_{in}$$

The potentiometer as shown above has three terminals Power (A), Ground (W) and Signal (B).

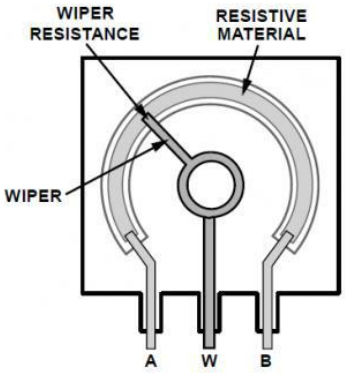

Fig (7.3) Voltage divider implementation in a POT (Source: Google images)

Arduino Uno: The orientation values from the 3-ROSM are pure analog variation in voltage. This variation in voltage has to be converted in to a Pulse Width Modulated (PWM) signal before it can be input in to the Servo motor. This crucial interface is played by a microcontroller. Our microcontroller of choice is the Arduino Uno. We chose the Uno as it was a very popular open source hardware platform with a very vibrant community of users built around it who could be leveraged to solve any problem.

Fig (7.4) Arduino Uno (Source: www.arduino.cc)

7.2. Procedure

Using the hollow core encoders to test the variation in values with the User input angle, the behaviour of the hollow core encoders were tested. Rotational input was given and the output was studied. This was also intended to test the Arduino Uno board. Wiring diagram:

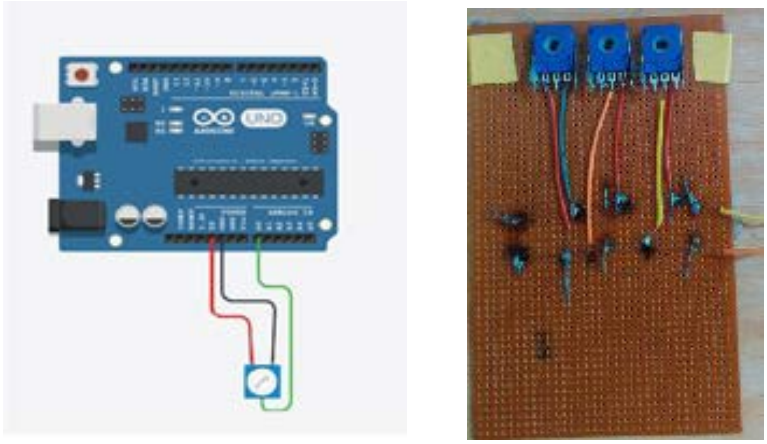

Fig (7.5) Wiring for testing encoders (ref: www.circuits.io)

Colour of the wire	Pin connected to
Green (Signal)	A0
Red (Power)	5V
Black (Ground)	GND

Table [7.2] Reference for the wiring in Fig (7.5)

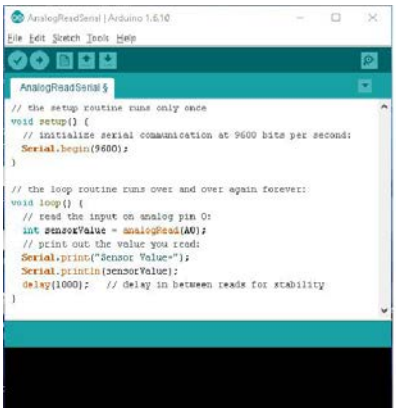

fig (7.6) Arduino code to check the encoder

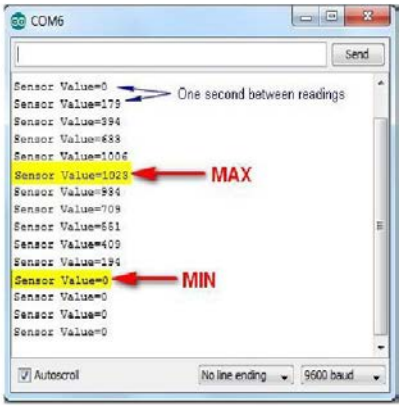

Fig (7.7) Output in Serial Monitor

Next the control of three Tower pro servo motors with three potentiometers were performed.

Wiring diagram (for testing):

Wire name	Pin number
A	6
B	5
C	3
D	A0
E	A1
F	A2

Table [7.3] Reference for wiring in Fig (7.8)

After testing the wiring of the encoders/servos, the encoders are mounted on the mechanism

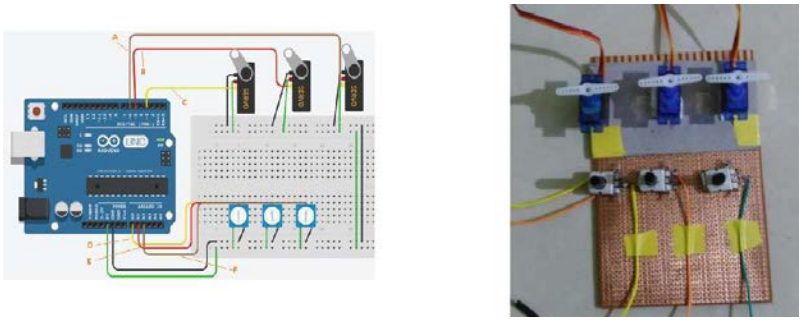

Fig (7.8) Wiring used during testing the servos

8.Application: Pan-Tilt-Roll Camera

The objective of this section is to fabricate a three axis camera mount that would visually demonstrate the output of the 3-ROSM. Also an additional requirement was to obtain one to one mapping of the input (orientation values) and the output. For the latter to happen, it had to be ensured that all motor axes (essentially three) intersected. In the process, two prototypes were created. The first prototype was made of mild steel L links. This was meant for us to act as a starting point to test the concept. Due to its weight, we ended up making a second prototype this time 3 d printing it in PolyLactic acid (PLA).

8.1 Component description:

Components used	Quantity
15-17kg torque Servo motor	3
L shaped links(3d printed PLA)	3
Base plate(3d printed PLA)	1
Web camera	1

Table [8.1] Component table

A servomotor is a rotary actuator that provides exact control of angular motion. It is able to precisely move to any angle between 0 and 180.This control is made possible by the encoder module that measures the angle of rotation of the DC motor it is attached to and provides position feedback. The input to its control is a signal (either analogue or digital) representing the position commanded for the output shaft. Servomotors are not a specific class of motor although the term servomotor is often used to refer to a motor suitable for use in a closed-loop control system.

In the simplest case, the encoder measures only the position. The measured position of the output is compared to the command position, the external input to the controller. If the output position differs from that required, an error signal is generated which then causes the motor to rotate in either direction, as needed to bring the output shaft to the appropriate position. As the positions approach, the error signal reduces to zero and the motor stops.

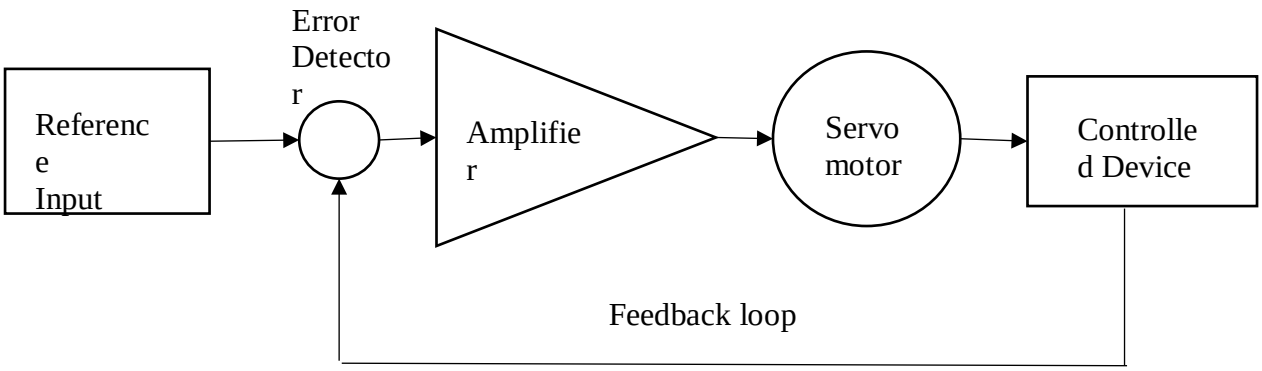

Fig (8.1) Servo system block diagram

Two sizes of Servo motors are being used in this project. The bottom and middle servo is the High Torque RC Servo Motor with metal gears and the top motor is the Tower Pro SG90 micro servo. The high torque motor has an operating torque of 15kg which is more than sufficient for the purposes of the project. However, a lower torque motor can also be used since the load to be carried is less than 1 kg.

Fig (8.2) High torque servo motor
(Source: www.nex-robotics.com)

Fig (8.3) Tower pro sg90
(Source: www.amazon.com)

Three L shaped links were used to transfer the motion from the servo motor to the web camera. In the first prototype, mild steel was used as the material. But owing to its weight, it was decided to be 3-D printed in PLA for the second prototype. The L shape was opted for its design simplicity and relatively low cost.

The Web camera is the device that is intended to be controlled by the mechanism. So a choice of camera model was made keeping in mind the cost and the image quality. After surveying the market, we ordered the Quantum QHM495LM Webcam. It weighs 380g.

Fig (8.4) Web camera (Source: www.amazon.com)

8.2 Communication between the encoders and servo motors

The orientation values extracted from the 3 ROSM is to be input in to the Servo motor. The trouble is that the motors have an output resolution of 8 bit (0-255) while the encoders are 10 bit (0-1023). So they cannot be directly input in to the servo motor.

The solution: To use an inbuilt function called map () to map the output values of the encoder to the output range of the servo motor. Once the values are mapped they can be input in to the servo motor using the SERVO library inbuilt in to the Arduino IDE. The servo library allows the Arduino board to interface with the servo motors. A specific library is required for servos as they don't operate only at two voltage levels namely 5V and Ground as does the DC motors. Their speed can be controlled by varying the input values over a range of voltage levels depending on the output resolution of the board which in this case is 8 bits. Thus we are able to vary the voltage in steps of (255-0)/ (5-0), i.e., 51V. This type of speed control is technically termed Pulse Width Modulation (PWM). This technique works essentially by varying the duty cycle of the signal being sent to the device, servomotor in this instance. A dc output is essentially a square wave, with the elevated part being the "HIGH" or 5v. The time for which the signal is high proportional to the time period of the signal is called the duty cycle. If the signal is high only for 50% of the time, then a sufficiently high frequency signal (say 500Hz) will produce half the speed in a servomotor. This way by controlling the duty cycle the speed of the motor can be controlled. Once the code is written, it is uploaded in to the Arduino Uno board.

Wiring diagram (Green wire-5V Black wire-GND)

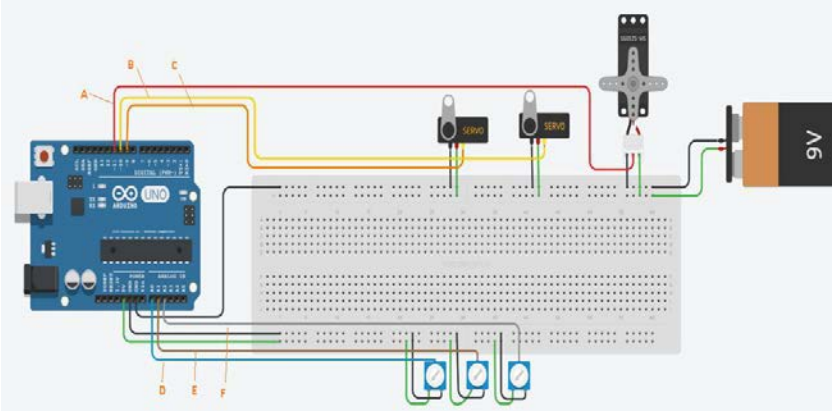

Fig (8.5) Final wiring diagram

Component name	Wire label	Pin name
Top servo(Tower pro)	A	11
Middle servo	B	10
Bottom servo	C	9
Bottom Encoder(controlling bottom motor)	D	A0
Middle Encoder(controlling middle motor)	E	A1
Top Encoder(controlling top motor)	F	A2

Table [8.2] Reference table for wiring in Fig (8.5)

8.3 Powering the servo motors

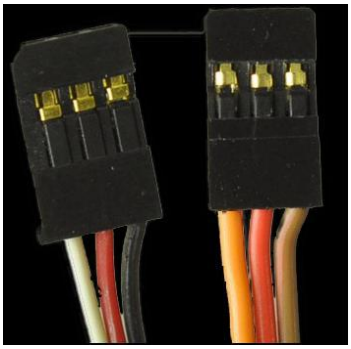

Fig (8.6) Servo terminals (Source: Google)

The white wire represents the signal, the red wire is the power input of 5V and the black wire is the grounding wire. The bottom and middle motors of the camera mount to be fabricated is the 15 kg torque RC Servo Motor with metal gears. They have an operating voltage rating of 5-12v. They have a stall current of 1000mA. Since the absolute maximum that each Input/output pin in Arduino can extract is 40 mA, the servos cannot be directly powered by the Arduino board. The Solution calls for an external power.

The servos normally work at 5v (can be pushed to 12v but with lot of noise and heat), but while working with them we mistakenly jammed one of it. As a result, it stopped running at 5v. Thus to work with it, the voltage had to be increased. After trial and error, the value of 9v was reached at. At 9 v, the motor operates with just a minor hum and minor heating effects. A 5V 2A (ampere) and a 9V 1A Adapter was purchased. The 5V adapter powered the bottom servo and the SG90 micro servo (top) and the 9V servo powered the middle servo. Two jumper wires were soldered together to positive terminal of the 5V adapter and one jumper wire soldered to that of 9V adapter. The negative terminals of both the adapter were connected together and soldered to four jumpers Wires-One each for the three servo motors and one to be connected to the Arduino board for maintaining a common ground.

8.4 Design and fabrication of Prototype I camera mount

The output of the 3 ROSM can be used in all applications which requires the remote control of orientation of an object of interest. The applications could be (but not limited to) a joystick for a CCTV unit, as an intuitive controller of an Industrial Arm End

Effector(EE) or as master slave system to handle radioactive materials in a nuclear power plant.

For the purpose of demonstration, it was decided to design and fabricate a camera mount which would provide a 1 to 1 mapping of the user input to the position of the object of interest which in this case is the camera.

Some of the commercially available options are listed below:

1		Fatshark 3-axis Camera Mount System	Rs 3222.3
2.		Tarot gopro t4 3 axis camera mount	Rs 14500
3		Geocalla G4-3D 3 Axis camera mount	Rs. 7,605.34

Table [8.3] Cost table of commercial products (Source: Google)

The cost was evidently a major obstacle for prospective buyers that with the costs starting from Rs4000 and increasing greatly for different models. To finish the project within a decent budget, it was decided to design and fabricate the 3 axis camera mount.

Once we obtained the Orientation values from the 3-ROSM, it is intended to be used to control the orientation of a camera. For this, a one to one mapping of the input and output is desired, i.e., the servos should exactly mimic the orientation of the 3-ROSM. To hold the servos and most importantly, the camera rigidly, a camera mount has to be designed. The design (of camera mount) should be rigid, compact and light. To start off, it was important for us to demonstrate the working of the concept. Thus we started off with mild steel as a material for the camera mount. The choice was made mainly because of its easy availability in the mechanical workshop and its obvious strength. A 2mm sheet was chosen as it had the desired

Balance of weight and rigidity. The sheet metal operations like Bending and drilling were performed on it to obtain the required dimensions. The L shape was chosen for its rigidity and ease of fabrication. Two L-shaped links were designed in Autodesk Inventor 2015 to hold the high torque servo motors. A simple c clamp was created by bending 1mm thick sheet metal to hold down the top servo.

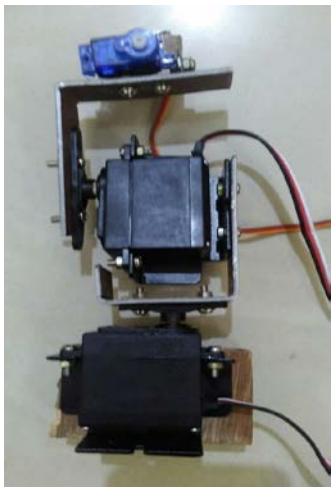

Fig (8.7) Camera mount prototype 1

The two L links were weighed just over 20g each and the C clamp weighed 5g. Thus the links alone weighed over 45g.Since all other components including servos, screws etc. will remain the same, weight reduction can only come out of these links. Thus the main drawback, so to say, was the weight factor. Also for one to one mapping of input and output, it was essential for three servo motor axes to intersect. But here, as is evident from Fig (8.7), they weren't intersecting. Another drawback with the design was the way

the top micro servo was mounted. It was strong enough to hold the motor, but its ability to also hold a web camera (at times vibrating) at various angles was doubtful.

8.5 Design and fabrication of Prototype II camera mount

The drawbacks of the first prototype was understood and addressed in the second and final prototype. Since weight reduction was the primary objective, it was decided to 3d print the L shaped links. They were to be printed in Polylactic acid or PLA. This material was chosen for the smooth surface finish and faster printing times it offered. Though cost wise, 3d printing was on the high side as opposed to just using mild steel, the weight reduction it offered more than made up for it. At about 5g each for the three links, they weighed 15g. The base plate which was also 3 d printed came at about 10g. Thus at about 25g, the weight reduction is significant. The one to one mapping was taken care of during the design of the L links. The three L-shaped links as before was designed in Autodesk Inventor 2015.

Fig (8.8) The mount after assembly

Fig (8.9) The mounted camera being controlled by the 3-ROSM

Their CAD design snapshots are as follows

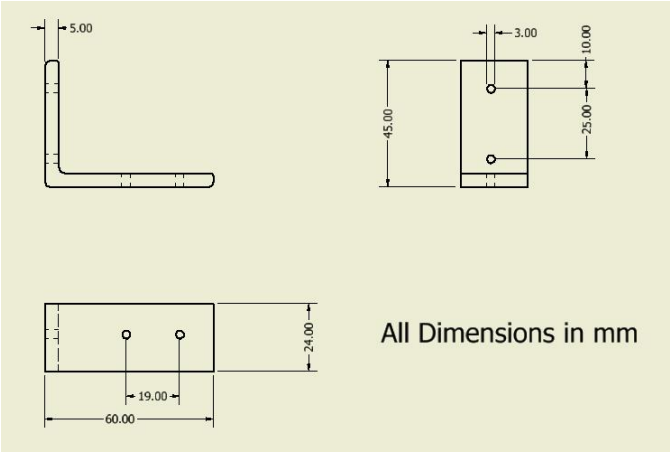

Fig (8.10) Bottom link

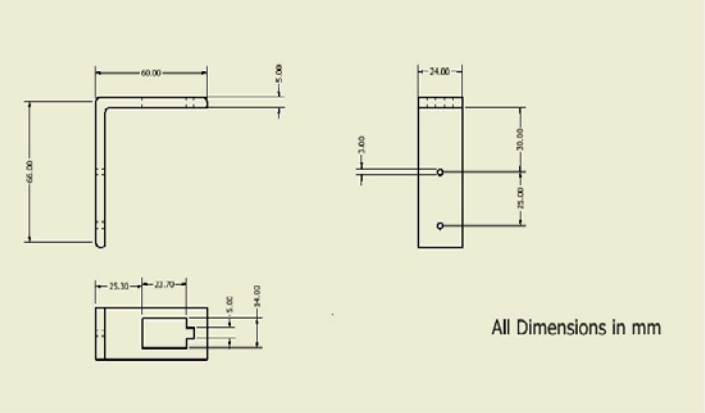

Fig (8.11) Middle link

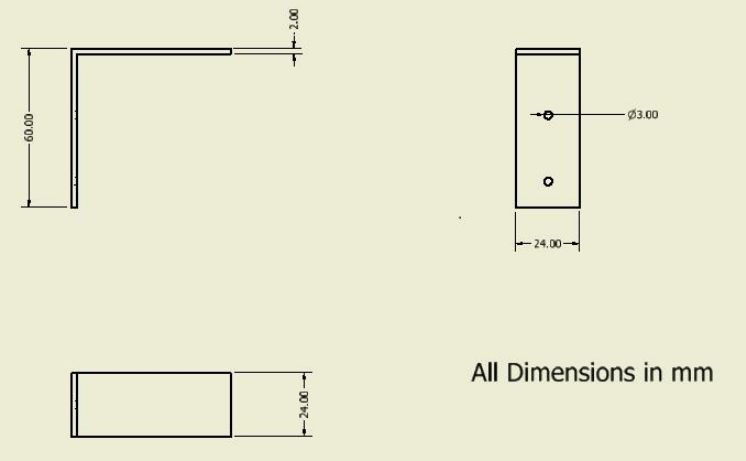

Fig (8.12) Top link

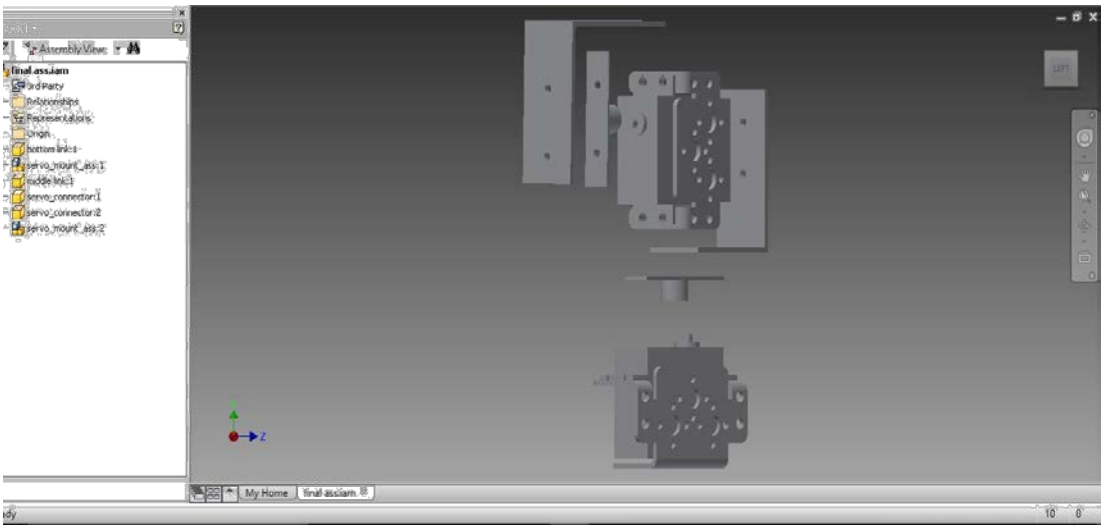

Fig (8.13) Exploded view of the final assembly

To provide 1:1 mapping, it was essential that all three axes intersect. For that, first the assembly window respective axes of the bottom and middle servos were made visible. Since their dimensions were not equal, their axes did not intersect on assembly. Thus a trial and error approach was followed to position the servo horn on the links. Finally, they intersected. Then the point of intersection was chosen and a point was created. Then an axis passing through the point and perpendicular to the top plane (of middle link) was created. This axis became the axis of the third motor. The cost of making the camera mount is listed below. The additional cost of the Webcam is Rs 415.

Part	Quantity	Cost(Rupees)
Bottom Link	1	119.40
Camera Bracket	1	138.59
Middle link	1	81
High torque Servo motor	2	2000
Tower Pro SG90 servo motor	1	110
Base plate	1	303
Total		2751.99

Table [8.4] The cost of various parts of the camera mount

8.6 Summary

Finally, the completed 3-axis motorized camera mount is linked to the 3-ROSM via the hollow bore encoders. These encoders are programmed offline, so that when there is a change in orientation of the 3-ROSM, the data is recorded as a change in voltage. This information is then relayed to the motorized camera mount which then moves accordingly. The encoders can move through an angle of 300° whereas the servo motors can only move through 180°. Hence in order to use the available workspace efficiently, the motors are set up so that their range lies in the middle of the total available range of the encoders. This divides the workspace symmetrically so that the user does not find the movement strange which may reduce the intuitiveness between the user and the expected visual output.

Fig (8.14) The control of camera mount being tested (a & b)

9.Conclusion

Through the course of this project, a novel design for an Orientation Sensing Mechanism was proposed. The features of this mechanism is that it is a low cost, energy efficient, adaptable and versatile orientation sensing mechanism that does not utilize servomotors, but still provides a very intuitive feel for the user as the three joint axes of this mechanism intersect at a central point emulating a human wrist. This is normally seen in parallel orientation controlling mechanisms, but in this project it has been implemented onto a serial chain mechanism.

Passive balancing was applied to the 3-ROSM to prevent its reorientation due to the action of gravity. This was achieved through the use of counterweights which balance the moment about a joint axis by applying a counter moment force in two orthogonal directions. This is another feature of the 3-ROSM in which a problem of balance in 3 Dimensions has been reduced to two 2 Dimension balancing problems which are easy to solve. Passive balancing was first performed on a CAD model of the initial design of the 3-ROSM and was later successfully verified using the Dynamic Simulation Module of Autodesk Inventor.

Thereafter two physical prototypes were designed and fabricated to test the various aspects of the 3-ROSM. The first prototype helped understand the problem of finding the practical Centre of Gravity location of a body and also the challenges faced in the fabrication of a revolute joint, which involves eliminating play. A novelty offered in this prototype is the addition of threaded extensions for placement of counterweights. The thread allows for infinite resolution in placing the counterweights to account for the possibility of change in mass of the entire system, which could be desired or undesired by the user. The second prototype was a scaled down model of prototype I which was redesigned such that it was easy to assemble and disassemble as desired by the user and increased the portability of the 3-ROSM. This prototype employed the use of encoders and successfully controlled a 3 axis motorized camera mount, whose design emulates the 3-ROSM. This was done so that a 1:1 mapping of the change in joint angles of the 3-ROSM could be used as an input for the camera mount.

9.1. Future Work

The 3-ROSM can be used for further experiments which may involve change in its design architecture or its use in a variety of applications with change in conditions of its work environment. The presence of a singularity when the axis of Joint 3 merges with the axis of Joint 1 is acknowledged. This leads to the elimination of a Degree of Freedom of the mechanism and either the design should be modified or a provision for this singularity should be taken so that it is eliminated.

Future work regarding the physical prototypes would include a scaled up model which employs the use of encoders or similar devices to measure joint angles. Prototype II can then be used to change the viewpoint of a virtual model in a CAD software. In the present model, there is a 1:1 mapping of the change in joint angles which in future can be changed to allow larger motion (operation of Heavy machinery) or small accurate changes in configuration. Prototype I provides a platform for the development of encoders that can accommodate a larger shaft size while not compromising on the accuracy of mapping the change in orientation.

10.References

[1] Antao, S.A , ; S. Vishal, ; Rajan, S. ; Nair, V. ; Chittawadigi, R.G. : Passive Balancing of a 3-R Orientation Sensing Mechanism. In The 8th asian conference on multibody dynamics ACMD, 2016.

[2] Arakelian V.: Gravity compensation in robotics. Advanced Robotics.; 30(2):79-96, 2016.

[3] Arakelian, V.: The history of the creation and development of hand-operated balanced manipulators (HOBM). In International Symposium on History of Machines and Mechanisms, pp. 347-356. Springer Netherlands, 2004.

[4] Arakelian,V.; Briot, S.: Balancing of Linkages and Robot Manipulators. Springer, 2015.

[5] Azadi, S.; Moradi, M.; Esmaili, A.: Optimal balancing of PUMA-Like robot in predefined path. Journal of Scientific & Industrial Research, 74, pp.209-211, 2015.

[6] Birglen, L. ; Gosselin, C. ; Pouliot, N. ; Monsarrat, B. ; Laliberte, T. : SHaDe, A New 3-DOF Haptic Device. *IEEE Transactions on Robotics and Automation*, 18(2): 166-175, 2002.

[7] Briot, S.; Arakelian, V.: A New Energy-free Gravity-compensation Adaptive System for Balancing of 4-DOF Robot Manipulators with Variable Payloads. In *T*he Fourteenth International Federation for the Promotion of Mechanism and Machine Science World Congress (2015 IFToMM World Congress), 2015.

[8] Brooks, T ; Bejczy, A : Hand controllers for teleoperation. JPL publications, 1985.

[9] Cheng, Z.; Foong, S.; Sun, D.; Tan, U. X.: Towards a multi-DOF passive balancing mechanism for upper limbs. In Rehabilitation Robotics (ICORR), 2015 IEEE International Conference *on* (pp. 508-513). IEEE, 2015.

[10] Deepak, S.: Static balancing of rigid-body linkages and compliant mechanisms. PhD diss., PhD. dissertation, 2012.

[11] Gosselin, C.: Gravity compensation, static balancing and dynamic balancing of parallel mechanisms. In Smart Devices and Machines for Advanced Manufacturing, pp. 27-48. Springer London, 2008.

[12] Jelatis, D. : Characteristics and evaluation of Master-slave manipulators. In Performance evaluaItion of Programmable Robots and Manipulators. NBS special publication, 1976.

[13] Koizumi, T. ; Tsujiuchi, N. ; Mori, K. ; Shibayama, T. : Identification of the Center-of-Gravity and Inertia Terms of 3-Dimensional Body. *Proceedings of the IMAC-XXV Conference & Exposition on Structural Dynamics*, Orlando, Florida, 2007.

[14] Kucuk, S. ; Bingul, Z. : Robot Kinematics : Forward and Inverse kinematics. In Industrial Robotics : Theory, Modelling and Control, Sam Cubero, INTECH, 2006.

[15] Lessard, S.; Bonev, I. A.; Bigras, P.; Briot, S.; Arakelyan, V.: Optimum static balancing of the parallel robot for medical 3D-ultrasound imaging. In IFTOMM 2007: 12th World Congress in Mechanism and Machine Science, 2007.

[16] Rahman, T.; Ramanathan, R.; Seliktar, R.; Harwin, W.: A simple technique to passively gravity-balance articulated mechanisms.Transactions-American Society Of Mechanical Engineers Journal Of Mechanical Design, *117*, pp.655-657, 1995.

[17] Saha, S. K. : Introduction to Robotics. Tata Mc-Graw Hill, 2014.

[18] Sheridan, T. B. (Ed.).: Performance Evaluation of Programmable Robots and Manipulators: Report of a Workshop Held at Annapolis, Md., Oct. 23-25, 1975. US Government Printing Office, 1976.

[19] Sheridan, T.B.; Ottensmeyer, M.; Kim, S.: Human-computer cooperation and intervention in telesurgery. Robotics and autonomous systems, 18(1), pp.127-134, 1996.

[20] Suthar, B. ; Zubair, M. ; Kansal, S. ; Mukherjee, S. : Haptics exoskeleton for tele-operation of Industrial robot. In The 3rd Joint International and the 7the Asian Conference on Multibody System Dynamics, 2014.

[21] Tsumaki, Y. ; Naruse, H. ; Nenchev, D. ; Uchiyama, M. : Design of a compact 6-DOF Haptic Interface,"Proceedings of the IEEE International Conference on Robotics and Automation, Leuven, Belgium, pp.2580-2585, May 1998.

[22] van der Wijk, V.; Herder, J. L.: Guidelines for low mass and low inertia dynamic balancing of mechanisms and robotics. In Advances in Robotics Research (pp. 21-30). Springer Berlin Heidelberg, 2009.

[23] Whitney, J. P.; Hodgins, J. K.: A passively safe and gravity-counterbalanced anthropomorphic robot arm. In Robotics and Automation (ICRA), 2014 IEEE International Conference on (pp. 6168-6173). IEEE, 2014.

[24] Yoon, J. ; Ryu, J. : Design, fabrication, and evaluation of a new haptic device using a paralel mechanism. In IEEE/ASME Transactions on Mechatronics, vol. 6, No.3, September, 2001

[25] Zhang, D.; Bin W.: Dynamic Balancing of Mechanisms and Synthesizing of Parallel Robots. Springer, 2015.